Atmos. Chem. Phys. Discuss., 13, 16961–17019, 2013
www.atmos-chem-phys-discuss.net/13/16961/2013/
doi:10.5194/acpd-13-16961-2013

Atmospheric Chemistry and Physics Discussions
Open Access

The direct and indirect radiative effects of biogenic secondary organic aerosol

C. E. Scott[1], A. Rap[1], D. V. Spracklen[1], P. M. Forster[1], K. S. Carslaw[1], G. W. Mann[1,2], K. J. Pringle[1], N. Kivekäs[3], M. Kulmala[4], H. Lihavainen[3], and P. Tunved[5]

[1]School of Earth and Environment, University of Leeds, Leeds, LS2 9JT, UK
[2]National Centre for Atmospheric Science, University of Leeds, Leeds, LS2 9JT, UK
[3]Finnish Meteorological Institute, Erik Palmenin aukio 1, 00560 Helsinki, Finland
[4]Department of Physics, University of Helsinki, P.O. Box 64, 00014, Finland
[5]Department of Applied Environmental Research, Stockholm University, Svante Arrhenius Väg 8c, 10691 Stockholm, Sweden

Received: 13 May 2013 – Accepted: 11 June 2013 – Published: 26 June 2013

Correspondence to: C. E. Scott (pm08c2s@leeds.ac.uk)

Published by Copernicus Publications on behalf of the European Geosciences Union.

Abstract

We use a global aerosol microphysics model in combination with an offline radiative transfer model to quantify the radiative effect of biogenic secondary organic aerosol (SOA) in the present day atmosphere. Through its role in particle growth and ageing, the presence of biogenic SOA increases the global annual mean concentration of cloud condensation nuclei (CCN; at 0.2 % supersaturation) by 3.6–21.1 %, depending upon the yield of SOA production, and the nature and treatment of concurrent primary carbonaceous emissions. This increase in CCN causes a rise in global annual mean cloud droplet number concentration (CDNC) of 1.9–5.2 %, and a global mean first aerosol indirect effect (AIE) of between $+0.01\,\mathrm{W\,m^{-2}}$ and $-0.12\,\mathrm{W\,m^{-2}}$. The radiative impact of biogenic SOA is far greater when it also contributes to particle nucleation; using two organically-mediated mechanisms for new particle formation we simulate global annual mean AIEs of $-0.22\,\mathrm{W\,m^{-2}}$ and $-0.77\,\mathrm{W\,m^{-2}}$. The inclusion of biogenic SOA substantially improves the simulated seasonal cycle in the concentration of CCN sized particles observed at three forested sites. The best correlation is found when the organically-mediated nucleation mechanisms are applied, suggesting that the AIE of biogenic SOA could be as large as $-0.77\,\mathrm{W\,m^{-2}}$. The radiative impact of SOA is sensitive to the presence of anthropogenic emissions. Lower background aerosol concentrations simulated with anthropogenic emissions from 1750 give rise to a greater fractional CCN increase and a more substantial indirect radiative effect from biogenic SOA. Consequently, the anthropogenic indirect radiative forcing between 1750 and the present day is sensitive to assumptions about the amount and role of biogenic SOA. We also calculate an annual global mean direct radiative effect (DRE) of between $-0.08\,\mathrm{W\,m^{-2}}$ and $-0.78\,\mathrm{W\,m^{-2}}$ in the present day, with uncertainty in the amount of SOA produced from the oxidation of biogenic volatile organic compounds (BVOCs) accounting for most of this range.

ACPD
13, 16961–17019, 2013

1 Introduction

Vegetation emits biogenic volatile organic compounds (BVOCs), such as monoterpenes ($C_{10}H_{16}$) and isoprene (C_5H_8), into the atmosphere (Guenther et al., 1995). Once emitted, BVOCs oxidise to yield a range of lower volatility oxidation products that can partition into the aerosol phase, forming secondary organic aerosol (SOA) (Kavouras et al., 1998; O'Dowd et al., 2002; Kanakidou et al., 2005; Jimenez et al., 2009). The oxidation products of monoterpenes and isoprene have been observed in both ambient aerosol (e.g. Kavouras et al., 1999; Yu et al., 1999b; Claeys et al., 2004; Robinson et al., 2011) and in laboratory chamber experiments (e.g. Hatakeyama et al., 1989; Edney et al., 2005; Kroll et al., 2005, 2006). Over Scandinavia, parcels of air have been found to contain an aerosol mass that is proportional to the length of time the air has spent over forested land (Tunved et al., 2006, 2008), suggesting an important contribution to aerosol from BVOC emissions.

Whilst organic aerosol has been shown to dominate the mass of fine aerosol over much of the world (Zhang et al., 2007; Jimenez et al., 2009), the climate effects of biogenic SOA are not well understood. The presence of SOA can influence the Earth's radiative balance by contributing to the absorption and scattering of radiation (the direct effect) and by altering the properties of clouds (indirect effects) (Forster et al., 2007). Incoming solar radiation peaks at wavelengths between 380 nm and 750 nm, so processes that aid in the growth of particles up to these sizes, such as the condensation of secondary organic material, will have a direct radiative effect (DRE). The annual global DRE from biogenic SOA has been previously estimated at between $-0.01\,\mathrm{W\,m^{-2}}$ (all-sky; Goto et al., 2008) and $-0.29\,\mathrm{W\,m^{-2}}$ (clear-sky; O'Donnell et al., 2011), but regional effects may be much larger e.g. summertime mean of between $-0.37\,\mathrm{W\,m^{-2}}$ and $-0.74\,\mathrm{W\,m^{-2}}$ over boreal regions (Lihavainen et al., 2009) and up to $-1\,\mathrm{W\,m^{-2}}$ over tropical forest regions (Rap et al., 2013).

The first aerosol indirect effect (AIE), or cloud albedo-effect, describes the radiative perturbation resulting from a change to the number concentration of cloud droplets,

ACPD
13, 16961–17019, 2013

when a fixed cloud water content is assumed (Twomey, 1977). This change is governed by the number of particles in the atmosphere that are able to act as cloud condensation nuclei (CCN), as determined by their size and chemical composition (Penner et al., 2001; Dusek et al., 2006). SOA formed from the oxidation products of isoprene and monoterpenes has been shown to be CCN active under atmospherically relevant conditions, with a hygroscopicity parameter close to 0.1 (Duplissy et al., 2008; Engelhart et al., 2008, 2011).

The presence of SOA can affect CCN number concentrations in several ways. Organic compounds are known to aid in the growth of newly formed particles (~ 1–2 nm diameter) to observable sizes (> 3 nm diameter; Boy et al., 2003; Kulmala et al., 2004; Verheggen et al., 2007; Laaksonen et al., 2008; Pierce et al., 2011; Yli-Juuti et al., 2011; Riccobono et al., 2012) and beyond, to a CCN-active size (>~ 70 nm diameter; Riipinen et al., 2011, 2012; Pierce et al., 2012; Paasonen et al., 2013). Additionally, the oxidation products of terpenes may play a role in the initial stages of particle formation, via stabilisation of the critical nucleus (Fan et al., 2006; Zhang et al., 2009; Metzger et al., 2010; Paasonen et al., 2010; Kulmala et al., 2013). In contrast, both laboratory (Kiendler-Scharr et al., 2009) and field experiments (Kanawade et al., 2011) indicate that isoprene emissions may act to suppress new particle formation in the presence of high isoprene to monoterpene emission ratios, although the mechanism through which this process operates is not known.

Several studies suggest a large first AIE from biogenic SOA over the boreal forests at high northern latitudes. Using a global aerosol microphysics model, Spracklen et al. (2008a) simulated a doubling of regional CCN concentrations as a result of monoterpene emissions, and a subsequent regional AIE of between −1.8 and −6.7 $W m^{-2}$ of boreal forest. A stronger annual AIE (locally between −5 and −14 $W m^{-2}$) was calculated by Kurten et al. (2003) using measurements taken at a boreal forest location in Finland. Globally, the AIE is weaker, and previous estimates range from negative to positive values. Rap et al. (2013) estimate a global annual mean AIE of −0.02 $W m^{-2}$ due to monoterpene SOA, and Goto et al. (2008) simulate an AIE (includ-

ACPD
13, 16961–17019, 2013

ing cloud lifetime and semi-direct effects) of $-0.19\,\mathrm{W\,m^{-2}}$. However, Goto et al. (2008) use an aerosol model that treats aerosol mass only, which is not ideal when examining processes that will influence the number size distribution (Bellouin et al., 2013). In contrast, O'Donnell et al. (2011) simulate a decrease in global mean CCN concentration and therefore a positive AIE of $+0.20\,\mathrm{W\,m^{-2}}$ for the emission of both biogenic and anthropogenic VOCs, potentially due to their differing microphysical treatment of SOA.

The aim of this study is to quantify the radiative effects of biogenic SOA in the present day atmosphere and examine the sensitivity to several important processes and parameters. We simulate changes in the global aerosol distribution resulting from the emission of BVOCs and calculate the DRE and first AIE. In order to examine the influence of present day anthropogenic emissions on the radiative effect of biogenic SOA, we also calculate the radiative effect of SOA in a pre-industrial atmosphere.

2 Method

2.1 Model description

The global aerosol microphysics model, GLOMAP (Spracklen et al., 2005b), is an extension to the TOMCAT global 3-D chemical transport model (Chipperfield, 2006). Here we use GLOMAP-mode (version 6), in which information about aerosol component masses and number concentrations is carried in five log-normal size modes (Mann et al., 2010, 2012): four hydrophilic (nucleation, Aitken, accumulation and coarse), and a non-hydrophilic Aitken mode. Material in the particle phase is classified into four components: sulphate (SU), black carbon (BC), particulate organic matter (POM) and sea-salt (SS). GLOMAP includes representations of nucleation, particle growth via coagulation, condensation and cloud processing, wet and dry deposition and in/below cloud scavenging.

The model has a horizontal resolution of $2.8^\circ \times 2.8^\circ$ with 31σ-pressure levels from the surface to 10 hPa. Meteorology is obtained from European Centre for Medium–

ACPD
13, 16961–17019, 2013

Range Weather Forecasts (ECMWF) reanalyses at six hourly intervals and cloud fields from the International Satellite Cloud Climatology Project (ISCCP) archive (Rossow and Schiffer, 1999). All simulations are performed for the year 2000, with six months spin-up from zero initial aerosol.

2.1.1 Gas phase emissions and chemistry

Monthly emissions of monoterpenes and isoprene are taken from the Global Emissions InitiAtive (GEIA) database (Guenther et al., 1995), giving total emissions of 127 and 503 Tg (C) yr^{-1}, respectively. Considerable variability is observed in the yield of SOA generated by BVOC oxidation (e.g. Yu et al., 1999a; Kroll et al., 2006; Shilling et al., 2009). Here we generate SOA at fixed molar yields of 13 % and 3 % (14.3 % and 3.3 % mass yield) for the oxidation of monoterpenes and isoprene respectively. Monoterpenes are prescribed the reaction characteristics of α-pinene, and oxidation reactions proceed at the rates given in Table 1. As a result of uncertainty in the SOA yield, as well as the magnitude of BVOC emissions and their rate of oxidation in the atmosphere, the global production of biogenic SOA remains poorly constrained, with estimates ranging between 12 Tg (SOA) yr^{-1} and 1820 Tg (SOA) yr^{-1} (Griffin et al., 1999; Kanakidou et al., 2005; Goldstein and Galbally, 2007; Heald et al., 2010, 2011; Spracklen et al., 2011b). Here we explore this uncertainty by varying the SOA production yield in a series of sensitivity experiments.

Global aerosol modelling studies commonly assume that the organic material generated by BVOC oxidation is either non-volatile (Spracklen et al., 2008a; Pierce and Adams, 2009; Makkonen et al., 2012) or semi-volatile (Pye and Seinfeld, 2010; O'Donnell et al., 2011). When semi-volatile products are partitioned with an equilibrium approach, organics are preferentially added to larger size particles with negligible particle mass added to smaller particles. However, organic oxidation products are observed in nucleation mode particles (Smith et al., 2008) and measurement-modelling studies suggest that their volatility is low (Pierce et al., 2011). Furthermore, newly formed particles do not grow to their measured sizes if organic oxidation products are assumed not

ACPD
13, 16961–17019, 2013

to partition to growing nuclei (Riipinen et al., 2011). In order to account for the growth of new particles, in this work we assume that BVOCs oxidise to form non-volatile organic material which condenses irreversibly onto existing aerosol according to their Fuchs–Sutugin corrected surface area (Fuchs and Sutugin, 1971). Sensitivity to the approach used for gas to particle partitioning is examined in another publication (Scott et al., 2013).

We prescribe six hourly mean offline oxidant (OH, O_3, NO_3, HO_2, H_2O_2) concentrations from a previous TOMCAT simulation (Arnold et al., 2005). GLOMAP also includes phytoplankton emissions of dimethyl-sulphide (DMS), calculated using monthly seawater DMS concentrations from Kettle and Andreae (2000), and gas-phase sulphur dioxide (SO_2) emissions from anthropogenic sources (Cofala et al., 2005), wildfires (van der Werf et al., 2004), and both continuous (Andres and Kasgnoc, 1998) and explosive (Halmer et al., 2002) volcanic eruptions.

2.1.2 Primary particulate emissions

Annual mean emissions of black carbon (BC) and particulate organic matter (POM) from fossil and bio-fuel combustion are taken from Bond et al. (2004), and monthly wildfire emissions are from the Global Fire Emissions Database (GFED) inventory (van der Werf et al., 2004). In a sensitivity study we use wildfire and anthropogenic emissions from the year 1750, compiled for the AeroCom initiative (Dentener et al., 2006). The emission of primary sea-salt aerosol is parameterised according to Gong (2003).

2.1.3 New particle formation

Since new particle formation has been shown to strongly affect CCN concentrations (Spracklen et al., 2008b) and simulated aerosol indirect radiative effects (Bellouin et al., 2013), we quantify the impact of BVOC emissions using four nucleation mechanisms. In all experiments we include binary homogeneous nucleation (BHN) of sulphuric acid and water (Kulmala et al., 1998a) which occurs mainly in the free troposphere (e.g.

ACPD
13, 16961–17019, 2013

Spracklen et al., 2005a). We also examine the impact of BVOC emissions when boundary layer nucleation is applied, in addition to BHN, using three different parameterisations from the literature. The first is an empirically derived mechanism for the activation (ACT) of sulphuric acid clusters in the boundary layer based on the work of Kulmala et al. (2006). With this approach, molecular clusters activate at a rate (J^*_{Act}) proportional to the gas phase concentration of sulphuric acid (Eq. 1). The coefficient A represents the complexity of the activation process and may be a function of several parameters such as temperature and the concentration of other species, potentially organics. Here we use a value for A of $2 \times 10^{-6}\,\mathrm{s}^{-1}$ (as determined empirically by Sihto et al., 2006) and restrict this mechanism to the boundary layer, allowing BHN to proceed at higher altitudes.

$$J^*_{\mathrm{Act}} = A[\mathrm{H_2SO_4}] \tag{1}$$

The final two parameterisations, Org1 (Eq. 2) and Org2 (Eq. 3) are implemented using the particle formation rates described by Metzger et al. (2010) and Paasonen et al. (2010) respectively ($k = 5 \times 10^{-13}\,\mathrm{s}^{-1}$, $k_1 = 1.1 \times 10^{-14}\,\mathrm{s}^{-1}$, $k_2 = 3.2 \times 10^{-14}\,\mathrm{s}^{-1}$). In smog chamber experiments, Metzger et al. (2010) found that particle formation rates were proportional to the product of the gas-phase concentrations of sulphuric acid and low volatility products from the photo-oxidation of an SOA precursor species (1,3,5-trimethylbenzene). They also found that sub-3 nm particle growth rates were too high to be explained by sulphuric acid vapour alone, proposing that organic oxidation products were also required to explain the observations. Paasonen et al. (2010) found good correlation against a wide observational dataset when the particle formation rate combined a term based on the product of the concentrations of sulphuric acid and an organic molecule, and a kinetic nucleation term proportional to the square of sulphuric acid concentration. When implementing these two organic-mediated nucleation mechanisms, we include only the product from monoterpene oxidation as the organic oxidation product, since the role of isoprene oxidation products in new particle formation remains unclear. Our experiments therefore apply these two nucleation rate parame-

ACPD
13, 16961–17019, 2013

terisations (Eqs. 2, 3), throughout the atmosphere, using the first stage product from monoterpene oxidation as the condensable organic species, org:

$$J^*_{\mathrm{Org1}} = k\,[\mathrm{H_2SO_4}][\mathrm{org}] \tag{2}$$

$$J^*_{\mathrm{Org2}} = k_1[\mathrm{H_2SO_4}]^2 + k_2\,[\mathrm{H_2SO_4}][\mathrm{org}] \tag{3}$$

The growth of newly formed clusters is not simulated explicitly, but the production rate, J_m, of particles at a measurable size (taken as $d_m = 3\,\mathrm{nm}$) is calculated using the approximation of Kerminen and Kulmala (2002), as given in Eq. (4). The cluster dry-diameter, d^*, is taken as 0.8 nm for J^*_{Act}, 1.5 nm for J^*_{Org1} (Metzger et al., 2010), and 2 nm for J^*_{Org2} (Paasonen et al., 2010).

$$J_m = J^* \exp\left\{0.23\left[\frac{1}{d_m} - \frac{1}{d^*}\right]\frac{\mathrm{CS}'}{\mathrm{GR}}\right\} \tag{4}$$

This production rate accounts for scavenging by larger particles, and allows growth of nucleated clusters up to d_m at a constant rate, GR, proportional to the gas phase concentration sulphuric acid. The reduced condensation sink, CS′, is calculated by integrating over the aerosol size modes following Kulmala et al. (2001b).

2.2 Model experiments

To examine the extent to which the simulated climate impacts of biogenic SOA are sensitive to our model's treatment of aerosol processes, we completed the series of model experiments described in Table 2. These simulations explore the impact of uncertainty in the SOA yield from BVOC oxidation, the role of organic oxidation products in new particle formation, and the interaction between SOA and primary carbonaceous aerosol emissions. To account for the uncertain yield of SOA produced by the oxidation of BVOCs, we varied the SOA mass yields by different factors (Expt. 5 to 7), resulting in a global annual production of between 18.5 Tg(SOA) yr^{-1} and 185.0 Tg(SOA) yr^{-1}. The

ACPD
13, 16961–17019, 2013

global annual production of SOA from these yield experiments is detailed in Table 2 and all lie within the wide range of previous estimates (Griffin et al., 1999; Kanakidou et al., 2005; Goldstein and Galbally, 2007; Heald et al., 2010, 2011; Spracklen et al., 2011b).

In GLOMAP, the simulated aerosol size distributions and therefore CCN concentrations, are sensitive to the treatment of primary anthropogenic emissions (Reddington et al., 2011; Spracklen et al., 2011a), in particular the emission characteristics of primary carbonaceous aerosol. Here, we emit primary carbonaceous particles with the distribution characteristics described by Stier et al. (2005) in our standard simulations, i.e. number median diameter $D_{ff} = 60$ nm and $D_{bf} = 150$ nm, standard deviation $\sigma_{ff} = 1.59$ and $\sigma_{bf} = 1.59$ (where ff = fossil fuel and bf = biofuel/wildfire respectively). We explore the sensitivity to this choice with an additional set of simulations (Expts. 11 and 12) using the smaller emission size ($D_{ff} = 30$ nm, $D_{bf} = 80$ nm), but wider distribution ($\sigma_{ff} = 1.8$, $\sigma_{bf} = 1.8$) recommended by AeroCom (Dentener et al., 2006).

The process of physical ageing, by which non-hydrophilic particles become hydrophilic via condensation of soluble material, is poorly understood (Kanakidou et al., 2005). In GLOMAP, we emit primary BC/OC particles into a non-hydrophilic distribution and transfer these particles to an internally mixed hydrophilic distribution after the condensation of a specific amount of condensable material. Our standard simulations assume that ten monolayers of condensable material (secondary organics or sulphuric acid) are required to sufficiently coat an insoluble particle for it to become soluble. To examine the importance of this process, and its representation with respect to the impact of biogenic SOA, we perform one simulation in which physical ageing does not occur as a result of the condensation of secondary organics (Expt. 8), and others in which only one soluble monolayer is required (Expts. 9 and 10).

The sensitivities examined here are not intended to provide an exhaustive assessment of the uncertainty associated with the radiative impact of biogenic SOA, but to highlight the importance of several key parameters in determining the direct and indi-

ACPD
13, 16961–17019, 2013

rect effects. A more thorough assessment of sensitivities and feedbacks would require an emulator-style approach (e.g. Lee et al., 2012) to model the entire parameter space.

2.3 Calculation of CCN concentrations

CCN concentrations were calculated offline, from monthly-mean aerosol tracers, using the approach of Petters and Kreidenweis (2007). A hygroscopicity parameter (κ) is assigned to each component; a multicomponent κ_{multi} is then obtained by weighting the individual κ values by the volume fraction of each component. We assign the following individual hygroscopicity parameters: sulphate (0.61, assuming ammonium sulphate), sea-salt (1.28), black carbon (0.0), and particulate organic matter (0.1). Whilst there is uncertainty associated with the hygroscopicity parameter for organic material in the atmosphere due to the wide range of solubilities observed, κ values close to 0.1 have been reported for secondary organic components (Engelhart et al., 2008, 2011; Gunthe et al., 2009; Dusek et al., 2010; King et al., 2010), and the entire organic fraction (Wang et al., 2008; Chang et al., 2010). We calculate CCN concentrations at a supersaturation of 0.2 % which is equivalent to an activation dry diameter of approximately 80 nm (assuming a composition of pure ammonium sulphate). We assume that BC/OC particles in the non-hydrophilic distribution do not act as CCN.

2.4 Cloud droplet number concentration

Cloud droplet number concentrations (CDNC) are calculated using the parameterisation of Nenes and Seinfeld (2003), as updated by Fountoukis and Nenes (2005) and Barahona et al. (2010). The monthly-mean aerosol size distribution is converted to a supersaturation distribution from which the number of activated particles can be determined for the diagnosed maximum supersaturation (S_{max}). The S_{max} of an ascending cloud parcel represents the competition between increasing water vapour saturation with decreasing temperature, and the loss of water vapour through condensation onto activated particles. As such, S_{max} depends upon the aerosol population and should be

ACPD
13, 16961–17019, 2013

diagnosed rather than prescribed uniformly, as discussed by Pringle et al. (2009). Here, CDNC are calculated with a prescribed constant updraught velocity of 0.15 $m\,s^{-1}$ over sea and 0.3 $m\,s^{-1}$ over land, consistent with those commonly observed for low-level stratus and stratocumulus clouds (Guibert et al., 2003; Peng et al., 2005; Pringle et al., 2012).

2.5 Radiative effects

The DRE and first AIE of biogenic SOA are determined using the offline radiative transfer model of Edwards and Slingo (1996) with nine bands in the longwave and six bands in the shortwave. We use a monthly mean climatology based on ECMWF reanalysis data, together with cloud fields from the ISCCP-D2 archive (Rossow and Schiffer, 1999) for the year 2000. Sensitivity of direct and first indirect radiative effects to the cloud climatology used (i.e. single year versus multi-annual mean) was examined in Rap et al. (2013) and found be to be negligible for a range of natural aerosol sources including monoterpene derived SOA.

To determine the DRE, following the methodology described in Rap et al. (2013), the radiative transfer model was used to calculate the difference in net top-of-atmosphere (SW + LW) all-sky radiative flux between experiments including SOA and the equivalent experiments without SOA. Aerosol scattering and absorption coefficients together with asymmetry parameters are calculated for each aerosol size mode and spectral band, as described in Bellouin et al. (2013).

The AIE is calculated as in Schmidt et al. (2012); a uniform control cloud droplet effective radius (r_{e1}) of 10 µm is assumed to maintain consistency with the ISCCP cloud data, and for each perturbation experiment the effective radius (r_{e2}) is calculated as in Eq. (5), from cloud droplet number fields $CDNC_1$ and $CDNC_2$ respectively. For each experiment, $CDNC_1$ represents the simulation including SOA, and $CDNC_2$ represents

ACPD
13, 16961–17019, 2013

the simulation with no SOA.

$$r_{e2} = r_{e1} * \left[\frac{\mathrm{CDNC}_1}{\mathrm{CDNC}_2}\right]^{\frac{1}{3}} \quad (5)$$

The first AIE of biogenic SOA is then calculated by comparing net (SW + LW) radiative fluxes using the varying r_{e2} values derived for each perturbation experiment, to those of the control simulation with fixed r_{e1}. In these offline experiments, we do not calculate the second aerosol indirect (cloud lifetime) effect.

3 Results

3.1 Changes to total particle and CCN number concentrations

Table 2 reports the impact of biogenic SOA on simulated aerosol properties. SOA increases the condensation sink, potentially suppressing new particle formation and growth. This results in the global annual mean total particle (N_3; greater than 3 nm dry diameter) concentration being reduced by 7.9 % when monoterpene emissions are included with activation boundary layer nucleation (Expt. 2) and by 0.4 % when BHN is the only new particle formation mechanism (Expt. 14). In contrast, when organics contribute directly to nucleation (Exp. 16 and 18), a global annual mean increase in N_3 of between 22.0 % and 142.0 % is simulated. In these simulations, the additional nucleation caused by the presence of organics dominates the moderate reduction in N_3 due to the enhanced condensation sink.

In all the model configurations examined here, biogenic SOA increases the simulated global annual mean surface CCN concentration, with the relative enhancement ranging between 3.6 and 45.2 % (Table 2). The spatial distribution of changes to CCN concentration (Fig. 1) does not simply match the distribution of BVOC emissions due to the diverse range of processes controlling the aerosol size distribution and CCN number. For the ACT simulation shown in Fig. 1, biogenic SOA (from monoterpenes and

ACPD
13, 16961–17019, 2013

isoprene) increases annual mean CCN concentrations by up to 120 % over the Amazon, whilst reducing annual mean CCN concentrations by up to 8 % over some tropical oceans.

The largest increases in absolute CCN concentration are simulated in regions coincident with primary particle emissions (particularly regions of tropical biomass burning) suggesting an important interaction between SOA and primary particles. In our model, primary carbonaceous aerosol from fossil fuel combustion and wildfire is initially non-hydrophilic, being emitted into the Aitken insoluble mode. Condensation of soluble gas phase species moves these particles into the hydrophilic Aitken mode, where they are able to act as CCN. Without this physical ageing by SOA, the global annual mean increase in CCN concentration is reduced to 3.6 % (Expt. 8), compared to 12.8 % in the equivalent standard run (Expt. 4). When the physical ageing requires only one monolayer of soluble material (Expt. 10), the global mean increase in CCN number concentration is reduced to 8.9 % because carbonaceous particles are more efficiently coated and transferred to the hydrophilic distribution by sulphuric acid, such that CCN concentrations are less sensitive to the presence of organics. Using a smaller emission size for primary carbonaceous aerosol (Expt. 12) increases the global annual mean change to surface CCN concentrations when biogenic SOA is included to 17.5 %. A smaller emission size increases the number of primary particles emitted per mass of carbonaceous material, thereby providing more non-hydrophilic particles ready to be aged to the hydrophilic modes where they are able to act as CCN. Additionally, the lower surface area of smaller particles allows a faster rate of ageing by a given amount of SOA.

At tropical latitudes (30° N to 30° S), high year-round emissions of both isoprene (87 % of global total emissions) and monoterpenes (78 % of total) result in large increases to CCN concentrations (Fig. 1) throughout the seasonal cycle (Fig. 2, left). At 30° N to 90° N, increases in CCN are largest during the summer, with small increases simulated in winter months when emissions of BVOC are low. Over the high latitude boreal forests, monoterpene emissions are responsible for the majority of the CCN increase (Fig. 2, left), owing to their higher emission rate compared to isoprene. In

ACPD
13, 16961–17019, 2013

the Southern Hemisphere (30–90° S), absolute CCN changes are small throughout the year due to low emissions of BVOC at these latitudes (Figs. 1, left and 2, left). However, relatively low absolute changes result in substantial fractional changes, particularly over the oceans (Fig. 1, right) due to low background CCN number concentration.

Within 30° either side of the equator, BVOC emissions from the GEIA inventory (Guenther et al., 1995) are slightly higher during the respective wet seasons (April–September in northern tropics; October–March in southern tropics), but as shown in Fig. 2 (right), the largest absolute increase in CCN concentration occurs during the dry seasons when primary carbonaceous emissions from wildfires are highest. The importance of ageing is confirmed by much lower CCN increase simulated when secondary organic material does not transfer hydrophobic particles to the hydrophilic distribution (dotted lines in Fig. 2, right). At high northern latitudes, the process of ageing also contributes to the summertime CCN increase (Fig. 2, right), but a more substantial contribution here comes from the growth of smaller particles to CCN active sizes via condensation of organic material.

BVOC emissions result in reductions in simulated CCN concentrations over some ocean regions (Fig. 1). Reductions in CCN are driven by two different processes. Firstly, the presence of biogenic SOA enhances the condensation sink over continental regions, resulting in increased condensation of sulphuric acid to existing particles. This can lower sulphuric acid concentrations in the upper troposphere, subsequently reducing binary homogeneous nucleation and the number of particles entrained into the boundary layer. This entrainment of particles formed in the upper troposphere makes the largest contribution to surface CCN concentrations over the sub-tropical oceans (Merikanto et al., 2009). Secondly, the presence of biogenic SOA allows non-hydrophilic particles to be aged (i.e. transferred to the hydrophilic distribution) and enhances their growth up to the size at which they may be nucleation scavenged (taken here as particles with dry diameter > 206 nm). In the absence of SOA, particle growth may only proceed via coagulation and condensation of sulphuric acid. Therefore in the presence of SOA, particles grow more quickly to a size where they may be removed

ACPD
13, 16961–17019, 2013

from the atmosphere by nucleation scavenging. Where these processes outweigh the generation of new CCN via particle growth, and ageing of primary particles, a net reduction in CCN concentration is simulated.

Monoterpene emissions contribute a greater increase to global annual mean CCN concentration, than isoprene emissions (Expt. 2 and Expt. 3; Table 2). This occurs partly because a greater amount of SOA is generated from their oxidation, despite total annual monoterpene emissions in the Guenther et al. (1995) dataset being a factor of four lower than those for isoprene, but may also be due to the spatial distribution of emissions and relative proximity to sources of fine particles that require growth to reach CCN sizes (e.g. carbonaceous particles from fossil fuel combustion). As indicated in Fig. 2 (left), the contributions of each BVOC are not additive; monoterpene and isoprene SOA increase CCN concentrations by approximately 10.4 % and 8.5 % respectively whereas the combined emission results in only 12.8 % increase, suggesting a saturation of the global CCN response. This is confirmed by the variation in CCN change observed for Experiments 4 to 7, where a factor of 5 increase in the SOA production yield results in less than a doubling of absolute and fractional CCN changes.

3.2 Sensitivity to new particle formation

The simulated contribution of SOA to global mean CCN concentrations depends strongly on the nucleation mechanism used in the model. Inclusion of an empirically derived particle activation mechanism within the boundary layer (i.e. ACT, Eq. 1) results in a greater absolute global annual change in CCN concentration due to monoterpene SOA (+23.5 cm^{-3}; Expt. 2), when compared to the equivalent simulation using only BHN (+20.3 cm^{-3}; Expt. 14). This occurs because particles formed by the activation of H_2SO_4 clusters in the boundary layer are able to grow to CCN active sizes by the condensation of organic oxidation products and is particularly evident between 40 and 60° N (Fig. 3, left) where there is a strong contribution to total particle numbers from nucleation within the boundary layer (Merikanto et al., 2009). However, a similar annual global mean fractional CCN change (+10.4 %) due to monoterpene SOA is simulated

ACPD
13, 16961–17019, 2013

in each case, owing to the higher background CCN concentration when the ACT mechanism is used.

When monoterpene oxidation products are allowed to participate directly in nucleation (Expts. 15 to 18), the contribution of biogenic SOA to CCN concentrations is substantially greater; increasing the global annual mean by 15.5 % for Org2 and 45.2 % for Org1. The large increase in CCN concentrations when the Org1 mechanism is used can be attributed to the fact that in the absence of BVOC emissions new particle formation in the boundary layer does not occur. With this mechanism, the peak annual mean absolute increase in CCN concentration occurs at approximately 40° N (Fig. 3, left) due to large CCN increases simulated over south east USA, Europe and China, regions of high monoterpene emission during the Northern Hemisphere summer. Substantial fractional increases (over 100 %) are simulated in regions where high monoterpene emissions combine with low background aerosol number concentrations such as the boreal regions of northern Russia and Canada (Fig. 3, right).

4 Comparison to observations

The simulated seasonal cycle in the number concentration of particles with dry diameter greater than 80 nm (N_{80}) was compared against multi-annual monthly mean observations at three forested sites: Hyytiälä, Finland (e.g. Kulmala et al., 1998b, 2001a) from 1996–2006, Pallas, Finland (e.g. Hatakka et al., 2003; Komppula et al., 2003) from 2000–2011, and Aspvreten, Sweden (e.g. Tunved et al., 2004) from 2005–2007. These locations were chosen since they are relatively remote from anthropogenic aerosol sources and are in regions with substantial BVOC emissions. We chose to evaluate N_{80} concentrations since these match particles of CCN relevant size. Although N_{80} does not take into account the composition or solubility of the particles, long-term observations of CCN are not yet available at any locations suitable for this study. Observations were taken from the EBAS database (available at http://ebas.nilu.no) and monthly mean model values are bi-linearly interpolated to each location.

ACPD
13, 16961–17019, 2013

Table 3 gives, for a selection of our experiments, the correlation coefficient (R) between simulated and observed monthly mean N_{80} concentrations at each site, and Fig. 4 shows the observed and simulated seasonal cycle at Hyytiälä and Pallas. A pronounced seasonal cycle in N_{80} is observed at these locations, with summertime (JJA) concentrations a factor of two greater than wintertime (DJF) concentrations. Without biogenic SOA, summertime N_{80} concentrations are under-predicted (dotted lines in Fig. 4) and simulations do not capture the seasonal cycle; the maximum correlation coefficient at Hyytiälä is 0.37 (Org2), 0.16 at Aspvreten (Org2), and 0.14 at Pallas (Org2). The inclusion of biogenic SOA improves the correlation between simulated and observed values for each set of simulations at all three locations, primarily by increasing summertime N_{80} concentrations.

When the ACT mechanism is used, increasing the yield of SOA production (Expt. 6 and 7) reduces the correlation coefficient at all three sites, when compared to the standard yield simulation (Expt. 4). This occurs because, at Hyytiälä for example, N_{80} concentrations simulated between June and September with the higher yields, are lower than simulated with the standard yield (not shown). During the summer months when BVOC emissions are highest, increasing SOA formation enhances the simulated condensation sink, suppressing new particle formation and growth of particles up to 80 nm. Varying the ageing of non-hydrophilic particles (Expt. 8 and 10) has little impact on seasonal cycles in N_{80} since both hydrophilic and non-hydrophilic particles contribute to the N_{80} concentration. The seasonal cycle is captured best when monoterpene oxidation products are included in the particle formation rate (red lines in Fig. 4), with the Org1 mechanism giving the best correlation at all three locations (0.61 at Hyytiälä, 0.46 at Aspvreten and 0.60 at Pallas).

We also compared simulated surface level CCN concentrations to a subset of the CCN dataset compiled by Spracklen et al. (2011a). The treatment of primary carbonaceous emissions has been shown to strongly influence particle number concentrations and aerosol size distributions simulated by global aerosol microphysics models (Reddington et al., 2011; Spracklen et al., 2011a). We therefore compared against measure-

ACPD
13, 16961–17019, 2013

ments filtered to minimise the influence of these particles: that is, data for terrestrial locations with a simulated present day/pre-industrial CCN concentration ratio (calculated from $[CCN]_{Expt.4}/[CCN]_{Expt.20}$) less than 2, during times when the site was reported to be unaffected by wildfire emissions. This subset of data contained 25 observations (each representing time weighted mean CCN concentration from a sampling period of days to weeks) from the 6 locations detailed in Table 4. Relative uncertainties in the observational dataset all lie in the range ± 5–40 %, but most within ± 10–20 %. CCN concentrations from the model were calculated for each of the 6 locations using the supersaturation at which the observations were recorded.

Table 3 reports normalised mean bias between observed and simulated CCN calculated according to Eq. (6) where S_i are CCN number concentrations simulated by the model, and O_i are observed CCN number concentrations at each location, i.

$$\mathrm{NMB} = 100\,\% \times \sum (S_i - O_i) \div \sum O_i \tag{6}$$

In the absence of biogenic SOA, CCN concentrations are under-predicted (NMB = −44.4 % for ACT, −48.6 % for Org1 and −26.6 % for Org2). Inclusion of biogenic SOA reduces the NMB at these locations, and to within the uncertainty associated with the observational dataset, e.g. from −44.4 % to −16.0 % with ACT. Whilst the inclusion of monoterpene emissions in the particle formation rate (Expts. 16 and 18) improved the correlation with the observed seasonal cycle at the European sites, simulations Org1 and Org2 lead to an over prediction (NMB = +16.9 % for Org1 and +20.0 % for Org2) of CCN concentration, but still within the uncertainty of the measurements.

When biogenic SOA is included, but is not able to age non-hydrophilic particles to the hydrophilic distribution, CCN concentrations are under-predicted (NMB = −40.5 %) suggesting that despite selecting for relatively pristine locations and times, the ageing of carbonaceous particles still contributes to local CCN concentrations. The faster rate of ageing makes little difference to the correlation (NMB = −16.5 %, as compared to −16.0 % for the standard ageing), suggesting that the process of generating CCN-active particles through physical ageing is not being limited by the availability of con-

ACPD
13, 16961–17019, 2013

densable material in these locations. This is confirmed by the narrow range of NMB values obtained for Exp. 4 to 7 (−16.0 to −17.2 %), over which the yield of SOA production is varied by a factor of 10. When the smaller emission size for BC/OC particles is used (Expt. 12), CCN concentrations are substantially over-predicted (NMB = +48.2 %), suggesting that this emission size generates too many CCN active particles in the presence of SOA.

5 Cloud droplet number concentrations

We simulate that biogenic SOA increases the global annual mean CDNC by between 1.9 % and 5.2 % when the ACT nucleation mechanism is used (Table 2). Figure 5 shows the spatial distribution of the annual mean change in CDNC due to the presence of biogenic SOA, when the ACT mechanism is used and emissions of both monoterpenes and isoprene are included. Over most regions, perturbations to calculated CDNC follow the same spatial pattern as changes to CCN concentration. However, in regions with high pre-existing aerosol concentrations, such as those heavily affected by biomass burning, activation of additional CCN to cloud droplets can become limited by competition for water vapour. This is evident over South America and western Africa, where the largest changes to CDNC (Fig. 5) do not coincide spatially with the largest changes to CCN (Fig. 1). As with CCN, relatively low absolute changes to CDNC in the Southern Hemisphere can lead to high fractional changes over the oceans. In the boreal regions, the inclusion of biogenic SOA increases the annual mean CDNC by up to 70 %, due to very low background CDNC and therefore a high sensitivity to additional CCN. Small decreases (< 10 %) in CDNC occur over the tropical oceans due to the decreases in CCN described in Sect. 3.1. As with CCN, including monoterpene oxidation products in the particle formation rate equation yields the greatest increase in CDNC due to biogenic SOA (26.6 % and 7.2 % for Org1 and Org2 respectively). Figure 6 shows the spatial distribution of the annual mean CDNC change when the Org1 mechanism is

ACPD
13, 16961–17019, 2013

used; as with CCN, large absolute increases are simulated at around 40° N, whilst fractional increases in excess of 100 % are simulated above 60° N (Fig. 3).

6 Radiative effect of biogenic SOA

We calculate a global mean DRE of between $-0.08\,\mathrm{W\,m^{-2}}$ and $-0.78\,\mathrm{W\,m^{-2}}$ for biogenic SOA in the present day atmosphere (Table 2), with the spatial distribution of the effect for Expt. 4 shown in Fig. 7 (left). Figure 8 (left) shows the sensitivity of the global annual mean direct effect to the processes examined in this study. The magnitude of the direct effect is highly sensitive to the amount of SOA (and therefore the amount of growth of particles) included in the simulation, with the global annual mean varying from $-0.09\,\mathrm{W\,m^{-2}}$ when the SOA production yield is halved (source of $18.5\,\mathrm{Tg(SOA)\,yr^{-1}}$), to $-0.78\,\mathrm{W\,m^{-2}}$ when the yield is increased by a factor of 5 (source of $185.1\,\mathrm{Tg(SOA)\,yr^{-1}}$). As such, the DRE is strongest over the tropics where BVOC emissions are highest (Fig. 7, left). Changes in the nucleation mechanism result in little variability in the DRE (range $-0.08\,\mathrm{W\,m^{-2}}$ to $-0.10\,\mathrm{W\,m^{-2}}$). The large increase in the number of nucleated particles and CCN simulated with the organic nucleation mechanisms is less important for the direct effect as these particles are too small to influence the path of incoming solar radiation. The DREs simulated by Rap et al. (2013) and O'Donnell et al. (2011) lie within the range we calculate here. Goto et al. (2008) calculated a smaller DRE of $-0.01\,\mathrm{W\,m^{-2}}$, but included less SOA ($\sim 7\,\mathrm{Tg(SOA)\,yr^{-1}}$), and used a mass-only aerosol model which does not simulate the growth of particles associated with the condensation of secondary organic material.

In the present day atmosphere, we calculate that biogenic SOA exerts a global annual mean first AIE of between +0.01 and $-0.77\,\mathrm{W\,m^{-2}}$ (Table 2). Figure 7 (right) shows the spatial distribution in the AIE due to biogenic SOA in a simulation using the ACT mechanism (Expt. 4). A negative AIE occurs in locations experiencing a large relative increase in CDNC (e.g. boreal Asia), or a modest increase in CDNC coinciding with a high fraction of low level cloud cover (e.g. Southern Hemisphere oceans). A positive

ACPD
13, 16961–17019, 2013

AIE occurs in locations where a small decrease in CDNC (Fig. 5) coincides with very high cloud fraction, such as the western coasts of Central America and Africa (Fig. 7, right).

Figure 8 (right) summarises the sensitivity of the global annual mean AIE to the processes examined in this study. The simulated global annual mean AIE is most sensitive to the nucleation mechanism used in the model (global annual mean range $-0.05\,\mathrm{W\,m^{-2}}$ to $-0.77\,\mathrm{W\,m^{-2}}$); the inclusion of monoterpene oxidation products in the particle formation rate results in greater CCN and CDNC increases, and therefore a more negative AIE, than either the BHN or ACT mechanisms. As with the ACT simulation, both organic nucleation mechanisms generate a negative AIE over the oceans between 30° S and 50° S, but Org1 in particular also yields large negative forcings in the Northern Hemisphere due to high fractional CCN and CDNC changes between 40° N and 60° N (Fig. 3).

Using the smaller size characteristics for primary carbonaceous emissions gives greater CCN and CDNC increases due to biogenic SOA, and subsequently a more substantial AIE of $-0.12\,\mathrm{W\,m^{-2}}$. When secondary organic material is not able to age non-hydrophilic particles to the hydrophilic distribution, the global annual mean AIE is reduced to $-0.02\,\mathrm{W\,m^{-2}}$, due to smaller increases in CCN and CDNC. Whilst increasing the yield of SOA production gives a greater global annual mean fractional increase in CDNC (Table 2), the increased yield enhances negative CDNC changes in regions with very high cloud fraction, so the AIE becomes less negative (e.g. $-0.04\,\mathrm{W\,m^{-2}}$ when the SOA yield is doubled).

Over boreal forests, regional annual AIEs of between $-0.1\,\mathrm{W\,m^{-2}}$ and $-0.5\,\mathrm{W\,m^{-2}}$ are calculated with the ACT mechanism (Fig. 7, right) and between $-0.1\,\mathrm{W\,m^{-2}}$ and $-1.5\,\mathrm{W\,m^{-2}}$ with the Org1 nucleation mechanism. As illustrated in Fig. 9, much of the boreal region experiences a summertime (JJA mean) of between $-1\,\mathrm{W\,m^{-2}}$ and $-5\,\mathrm{W\,m^{-2}}$, when the Org1 mechanism is used, matching the large cooling effect over these forest regions calculated by previous studies (Kurten et al., 2003; Spracklen et al., 2008a). However, the strongest radiative effects (up to $-9\,\mathrm{W\,m^{-2}}$) are simulated over

ACPD
13, 16961–17019, 2013

the adjacent ocean regions which experience smaller increases in CDNC but have higher cloud coverage (i.e. cloud fraction of 50–70 % as compared to 0–30 % over the land).

The AIE from monoterpene SOA ($-0.19\,\mathrm{W\,m^{-2}}$) estimated by Goto et al. (2008) lies within the range of AIE we calculate here. The AIE of $-0.02\,\mathrm{W\,m^{-2}}$ calculated by Rap et al. (2013) was for a GLOMAP simulation using BHN (as in our Expt. 14) and requiring only one soluble monolayer to transfer non-hydrophilic particles to the hydrophilic distribution (as in our Expt. 10), and is in line with the AIEs calculated here. O'Donnell et al. (2011) simulated a positive AIE ($+0.20\,\mathrm{W\,m^{-2}}$) for all SOA (i.e. biogenic plus anthropogenic), which lies outside our range (between +0.01 and $-0.77\,\mathrm{W\,m^{-2}}$). The positive AIE simulated by O'Donnell et al. (2011), may be caused by the secondary organic material being distributed preferentially amongst larger size particles (i.e. those already large enough to act as CCN), resulting in a decrease in global mean CDNC. We examine the sensitivity of the biogenic SOA AIE to assumptions concerning the part of the aerosol size distribution to which SOA is added (i.e. volatility treatment of the condensable material), in a further publication (Scott et al., 2013).

7 Sensitivity of the radiative effect of biogenic SOA to anthropogenic emissions

Primary particulate (POM and BC) and gas-phase (SO_2) emissions from anthropogenic sources were much lower in 1750 compared to the present day. These lower emissions result in lower simulated background (i.e. in the absence of biogenic SOA) concentrations of CCN. The radiative effect of biogenic SOA may therefore have been different in a pre-industrial atmosphere. To explore this possibility we simulated the impact of biogenic SOA in an atmosphere with 1750 anthropogenic emissions (Expt. 19 and 20; ACT_1750). Including biogenic SOA in a pre-industrial atmosphere yields a lower absolute change in CCN number concentration than in the present day. This lower absolute change is due to fewer ultrafine particles being available (from nucleation and primary sources) for growth to CCN sizes, or ageing, by the secondary organic material. De-

ACPD
13, 16961–17019, 2013

spite the lower absolute change, the inclusion of biogenic SOA results in a higher fractional change of +23.2 % (Table 2), due to lower background CCN concentrations in the pre-industrial atmosphere. This increased fractional change in CCN, combined with lower background CDNC results in a greater perturbation to CDNC due to biogenic SOA in a pre-industrial atmosphere (global annual mean +12.6 %, as compared to +4.4 % in the present day).

Since the fractional change in CDNC constrains the AIE (Eq. 5), a more substantial indirect effect of $-0.19\,\mathrm{W\,m^{-2}}$ is simulated with 1750 anthropogenic emissions (Expt. 20; ACT_1750) compared to $-0.06\,\mathrm{W\,m^{-2}}$ with the same model setup in the present day. Regions of both positive and negative change in CDNC are enhanced by the lower background concentration, so this global mean radiative effect represents a combination of Northern Hemisphere land and Southern Hemisphere ocean regions experiencing a more negative AIE and tropical oceans experiencing a more substantial positive AIE (Fig. 10), as compared to an equivalent simulation using present day anthropogenic emissions (Fig. 7, right).

The global mean AIE obtained using the Org1 particle formation mechanism (Expt. 22; Org1_1750) is also enhanced in the 1750 atmosphere ($-0.95\,\mathrm{W\,m^{-2}}$ as compared to $-0.77\,\mathrm{W\,m^{-2}}$ in the present day). The annual mean AIE is more negative at most latitudes, but at 30–50° S, the radiative effect is stronger in the present day simulation (full red line Fig. 10, right) due to higher SO_2 emissions in southern Africa and Australia, required to generate the H_2SO_4 needed to form new particles using the Org1 nucleation mechanism.

Increasing the SOA yield when 1750 anthropogenic emissions are used results in a greater fractional enhancement to CCN than when present day anthropogenic emissions are used (Fig. 11, left). This enhanced CCN sensitivity translates into a greater CDNC and AIE sensitivity and has implications for the first aerosol indirect radiative forcing (RF) due to anthropogenic aerosol emissions. To test this, we calculate an anthropogenic first indirect RF since 1750, by setting $CDNC_1$ in Eq. (5) to the present day, and $CDNC_2$ to the value obtained from a simulation using anthropogenic emis-

ACPD
13, 16961–17019, 2013

sions from 1750. We find that the first aerosol indirect RF from anthropogenic emission changes (1750 to present) is $-1.16\ \mathrm{Wm^{-2}}$ when we assume a low source of biogenic SOA ($18.5\ \mathrm{Tg(SOA)\,yr^{-1}}$) but decreases in absolute value to $-1.10\ \mathrm{Wm^{-2}}$ when we assume a large source ($185.1\ \mathrm{Tg(SOA)\,yr^{-1}}$) (purple circles in Fig. 11, right).

If the Org1 mechanism is used in both present day and 1750 simulations (red circle in Fig. 11, right), the calculated aerosol indirect RF is $-1.04\ \mathrm{Wm^{-2}}$, that is $0.12\ \mathrm{W\,m^{-2}}$ smaller than that derived using the ACT mechanism and an equivalent SOA source strength. The variation in first indirect anthropogenic RF, due to uncertainties in SOA yield and nucleation mechanism, highlights the need to understand the baseline pre-industrial atmosphere and the magnitude of pre-existing natural radiative effects in order to constrain the RFs due to human activities. A previous study demonstrated that uncertainty in volcanic SO_2 emissions plays a similar role in driving uncertainty in the anthropogenic first aerosol indirect RF (Schmidt et al., 2012).

In contrast, the DRE of biogenic SOA is less sensitive to the presence of anthropogenic emissions. When the ACT mechanism is used, the same DRE is simulated with present day and 1750 anthropogenic emissions ($-0.18\ \mathrm{W\,m^{-2}}$). When the Org1 mechanism is used, DREs of $-0.08\ \mathrm{W\,m^{-2}}$ and $-0.12\ \mathrm{W\,m^{-2}}$ are simulated with present day and 1750 anthropogenic emissions respectively. The DRE is slightly enhanced in the 1750 atmosphere because there is less organically-mediated new particle formation than in the present day (ΔN_3 is $+643.0\ \mathrm{cm^{-3}}$ in the present day, and $+437.3\ \mathrm{cm^{-3}}$ in the 1750 atmosphere), due to lower SO_2 emissions. As a result, there are fewer nucleation mode particles requiring condensable material for growth, in the 1750 atmosphere, and a greater proportion of the secondary organic material is distributed towards larger size particles which are capable of interacting with incoming radiation.

ACPD
13, 16961–17019, 2013

8 Summary and conclusions

We used a global aerosol microphysics model (GLOMAP) and an offline radiative transfer model to quantify the impact of biogenic SOA on CCN concentrations and CDNC, and the subsequent radiative implications.

In all present day simulations, the global annual mean CCN concentration increases (by between 3.6 % and 45.2 %) when biogenic SOA is included. In the absence of organic-mediated nucleation, most of the simulated increase in CCN number concentration occurs due to physical ageing, and subsequent growth, of non-hydrophilic particles originating from wildfire and carbonaceous combustion. However, when monoterpene oxidation products affect the new particle formation rate, CCN concentrations are mostly perturbed by the growth of newly formed particles to CCN active sizes. Similarly, at around 60° N, where monoterpene emissions are high during the Northern Hemisphere summer months, and background particle concentrations are low, a greater proportion of the CCN increase is associated with the growth of smaller particles. Regional decreases in CCN concentrations are simulated, in particular over the tropical oceans, due to both enhanced nucleation scavenging of non-hydrophilic particles, and the suppression of upper tropospheric nucleation. The spatial changes to CDNC from the inclusion of biogenic SOA broadly match changes to CCN concentrations, with global annual mean increases ranging from 1.9 % to 26.6 %. However, the magnitude of CDNC change becomes limited by competition for water vapour in highly polluted regions, such as those affected by biomass burning. The low sensitivity of CCN to the inclusion of biogenic SOA in experiments without organic-mediated nucleation is consistent with the much larger parameter sensitivity study of Lee et al. (2013). They varied biogenic SOA production between 5 and 360 Tg(SOA) yr^{-1}, which resulted in a global mean 3 % standard deviation in CCN concentration, with a maximum standard deviation of around 40 % locally. Our results confirm the suggestion of Lee et al. (2013) that organic-mediated nucleation would greatly increase the sensitivity of CCN to SOA.

ACPD
13, 16961–17019, 2013

The inclusion of biogenic SOA results in a present day global annual mean top-of-atmosphere DRE of between $-0.08\,\mathrm{W\,m^{-2}}$ and $-0.78\,\mathrm{W\,m^{-2}}$, and a first AIE of between $+0.01\,\mathrm{W\,m^{-2}}$ and $-0.77\,\mathrm{W\,m^{-2}}$. The DRE is most sensitive to the yield of SOA production and strongest in regions of high BVOC emission. Altering the yield of SOA production reduces the agreement with observations of particle number greater than 80 nm diameter (N_{80}) at 3 forested locations (Table 3), so our best estimate of the DRE from biogenic SOA is $-0.18\,\mathrm{W\,m^{-2}}$, consistent with global production of $37\,\mathrm{Tg(SOA)\,yr^{-1}}$. The largest uncertainty in the AIE of biogenic SOA comes from the representation of new particle formation in the boundary layer, specifically whether organic compounds contribute to the nucleation rate. Including the oxidation products of monoterpenes in the particle formation rate equation gives up to an 11 times greater AIE, from biogenic SOA, than when sulphuric acid alone controls new particle formation. The best agreement between simulated and measured seasonal cycles in N_{80} is obtained when monoterpene oxidation products affect the new particle formation rate, suggesting that the magnitude of the global annual mean AIE from biogenic SOA could lie towards the upper end of our estimated range of $-0.77\,\mathrm{W\,m^{-2}}$.

At high northern latitudes, monoterpene emissions from boreal forests result in summertime regional AIE of up to $-6\,\mathrm{W\,m^{-2}}$ over land, and $-9\,\mathrm{W\,m^{-2}}$ over ocean, when organic compounds influence the nucleation rate (Org1 mechanism). Previous studies (Betts, 2000; Snyder et al., 2004; Bala et al., 2007; Davin and de Noblet–Ducoudré, 2010) suggest that the low land-surface albedo of boreal forests exerts a warming (i.e. positive radiative effect) on the climate which potentially outweighs the cooling effect (i.e. negative radiative effect) due to carbon storage by these forests. Follow up work is required to examine the radiative effect of biogenic SOA in comparison to these other effects, in order to quantify the overall climate impact of boreal forests.

When the present day anthropogenic aerosol emissions in our simulations are replaced with those from 1750, the lower background aerosol concentrations result in a greater proportion of additional CCN becoming activated and therefore a more substantial AIE from biogenic SOA in the pre-industrial atmosphere ($-0.19\,\mathrm{W\,m^{-2}}$ and

ACPD
13, 16961–17019, 2013

$-0.95\,W\,m^{-2}$ for ACT and Org1 respectively). As such the AIE from biogenic SOA in 1750 is more sensitive to changes in the amount of SOA generated, and the nucleation mechanism used; adding uncertainty of $0.06\,W\,m^{-2}$ and $0.12\,W\,m^{-2}$ respectively to the magnitude of the first aerosol indirect RF from anthropogenic emissions since 1750 (Fig. 11, right).

As emissions of both biogenic and anthropogenic aerosol change in the future, our understanding of their effects and interactions will gain an increasing importance. Emissions of BVOCs will be sensitive to future changes in climate (e.g. Lathière et al., 2005; Tunved et al., 2008; Paasonen et al., 2013), vegetation, and carbon dioxide concentrations (Pacifico et al., 2012). Additionally, changes in the spatial distribution of BVOC emissions are likely to be as important as the global magnitude of emissions, as has been shown for changes to oceanic DMS emissions (Woodhouse et al., 2013).

Our results indicate that biogenic SOA very likely exerts a negative radiative effect in the present day climate, via both the direct and first indirect effect, and that the magnitude of these effects is highly sensitive to our understanding of SOA yield and aerosol microphysical processes. Our work also reinforces the need to fully understand the influences of natural components on the Earth system in order to accurately determine the radiative effects of human activities.

Acknowledgements. CES was supported by a Natural Environment Research Council (NERC) Doctoral Training Grant. AR is funded by NERC grant NE/J004723/1, DVS by NERC grant NE/G015015/1, PMF by Engineering and Physical Sciences Research Council (EPSRC) grant EP/I014721/1 and KSC by EC Seventh Framework Programme under grant agreement FP7-ENV-2010-265148 (Integrated Project PEGASOS). KSC and PMF are currently Royal Society Wolfson Merit Award holders. GMW and KSC are funded by the NERC National Centre for Atmospheric Science (NCAS). The Academy of Finland Centre of Excellence (FCoE) programme is acknowledged for supporting the observation programmes at Hyytiälä and Pallas (Project no. 1118615). The Swedish Environmental Agency (Naturvårdsverket) and Stockholm Environmental Protection Unit (Miljöförvaltningen) are acknowledged for providing financial support to the atmospheric observation programme at Aspvreten.

ACPD
13, 16961–17019, 2013

References

Andreae, M. O., Rosenfeld, D., Artaxo, P., Costa, A. A., Frank, G. P., Longo, K. M., and Silva-Dias, M. A. F.: Smoking rain clouds over the Amazon, Science, 303, 1337–1342, doi:10.1126/science.1092779, 2004.

Andres, R. J. and Kasgnoc, A. D.: A time-averaged inventory of subaerial volcanic sulfur emissions, J. Geophys. Res., 103, 25251–25261, doi:10.1029/98jd02091, 1998.

Arnold, S. R., Chipperfield, M. P., and Blitz, M. A.: A three-dimensional model study of the effect of new temperature-dependent quantum yields for acetone photolysis, J. Geophys. Res., 110, D22305, doi:10.1029/2005jd005998, 2005.

Atkinson, R., Baulch, D. L., Cox, R. A., Hampson, R. F., Kerr, J. A., and Troe, J.: Evaluated Kinetic and Photochemical Data for Atmospheric Chemistry: Supplement III: IUPAC Subcommittee on Gas Kinetic Data Evaluation for Atmospheric Chemistry Journal of Physical and Chemical Reference Data, 18, 881–1097, doi:10.1063/1.555832, 1989.

Atkinson, R., Baulch, D. L., Cox, R. A., Crowley, J. N., Hampson, R. F., Hynes, R. G., Jenkin, M. E., Rossi, M. J., Troe, J., and IUPAC Subcommittee: Evaluated kinetic and photochemical data for atmospheric chemistry: Volume II – gas phase reactions of organic species, Atmos. Chem. Phys., 6, 3625–4055, doi:10.5194/acp-6-3625-2006, 2006.

Bala, G., Caldeira, K., Wickett, M., Phillips, T. J., Lobell, D. B., Delire, C., and Mirin, A.: Combined climate and carbon-cycle effects of large-scale deforestation, P. Natl. Acad. Sci. USA, 104, 6550–6555, doi:10.1073/pnas.0608998104, 2007.

Barahona, D., West, R. E. L., Stier, P., Romakkaniemi, S., Kokkola, H., and Nenes, A.: Comprehensively accounting for the effect of giant CCN in cloud activation parameterizations, Atmos. Chem. Phys., 10, 2467–2473, doi:10.5194/acp-10-2467-2010, 2010.

Bellouin, N., Mann, G. W., Woodhouse, M. T., Johnson, C., Carslaw, K. S., and Dalvi, M.: Impact of the modal aerosol scheme GLOMAP-mode on aerosol forcing in the Hadley Centre Global Environmental Model, Atmos. Chem. Phys., 13, 3027–3044, doi:10.5194/acp-13-3027-2013, 2013.

Betts, R. A.: Offset of the potential carbon sink from boreal forestation by decreases in surface albedo, Nature, 408, 187–190, doi:10.1038/35041545, 2000.

Bond, T. C., Streets, D. G., Yarber, K. F., Nelson, S. M., Woo, J.-H., and Klimont, Z.: A technology-based global inventory of black and organic carbon emissions from combustion, J. Geophys. Res., 109, D14203, doi:10.1029/2003jd003697, 2004.

ACPD
13, 16961–17019, 2013

Boy, M., Rannik, Ü., Lehtinen, K. E. J., Tarvainen, V., Hakola, H., and Kulmala, M.: Nucleation events in the continental boundary layer: Long-term statistical analyses of aerosol relevant characteristics, J. Geophys. Res., 108, 4667, doi:10.1029/2003jd003838, 2003.

Chang, R. Y.-W., Slowik, J. G., Shantz, N. C., Vlasenko, A., Liggio, J., Sjostedt, S. J., Leaitch, W. R., and Abbatt, J. P. D.: The hygroscopicity parameter (κ) of ambient organic aerosol at a field site subject to biogenic and anthropogenic influences: relationship to degree of aerosol oxidation, Atmos. Chem. Phys., 10, 5047–5064, doi:10.5194/acp-10-5047-2010, 2010.

Chipperfield, M. P.: New version of the TOMCAT/SLIMCAT off-line chemical transport model: intercomparison of stratospheric tracer experiments, Q. J. Roy. Meteor. Soc., 132, 1179–1203, doi:10.1256/qj.05.51, 2006.

Claeys, M., Graham, B., Vas, G., Wang, W., Vermeylen, R., Pashynska, V., Cafmeyer, J., Guyon, P., Andreae, M. O., Artaxo, P., and Maenhaut, W.: Formation of secondary organic aerosols through photooxidation of isoprene, Science, 303, 1173–1176, doi:10.1126/science.1092805, 2004.

Cofala, J., Amann, M., Klimont, Z. S., and Schopp, W.: Scenarios of world anthropogenic emissions of SO_2, NO_x and CO up to 2030, in: Internal Report of the Transboundary Air Pollution Programme, International Institute for Applied Systems Analysis, Laxenburg, Austria, 2005.

Davin, E. L. and de Noblet-Ducoudré, N.: Climatic impact of global-scale deforestation: radiative versus nonradiative processes, J. Climate, 23, 97–112, doi:10.1175/2009JCLI3102.1, 2010.

Delene, D. J. and Deshler, T.: Vertical profiles of cloud condensation nuclei above Wyoming, J. Geophys. Res.-Atmos., 106, 12579–12588, doi:10.1029/2000jd900800, 2001.

Dentener, F., Kinne, S., Bond, T., Boucher, O., Cofala, J., Generoso, S., Ginoux, P., Gong, S., Hoelzemann, J. J., Ito, A., Marelli, L., Penner, J. E., Putaud, J.-P., Textor, C., Schulz, M., van der Werf, G. R., and Wilson, J.: Emissions of primary aerosol and precursor gases in the years 2000 and 1750 prescribed data-sets for AeroCom, Atmos. Chem. Phys., 6, 4321–4344, doi:10.5194/acp-6-4321-2006, 2006.

Duplissy, J., Gysel, M., Alfarra, M. R., Dommen, J., Metzger, A., Prevot, A. S. H., Weingartner, E., Laaksonen, A., Raatikainen, T., Good, N., Turner, S. F., McFiggans, G., and Baltensperger, U.: Cloud forming potential of secondary organic aerosol under near atmospheric conditions, Geophys. Res. Lett., 35, L03818, doi:10.1029/2007gl031075, 2008.

Dusek, U., Frank, G. P., Hildebrandt, L., Curtius, J., Schneider, J., Walter, S., Chand, D., Drewnick, F., Hings, S., Jung, D., Borrmann, S., and Andreae, M. O.: Size matters more

than chemistry for cloud-nucleating ability of aerosol particles, Science, 312, 1375–1378, doi:10.1126/science.1125261, 2006.

Dusek, U., Frank, G. P., Curtius, J., Drewnick, F., Schneider, J., Kürten, A., Rose, D., Andreae, M. O., Borrmann, S., and Pöschl, U.: Enhanced organic mass fraction and decreased hygroscopicity of cloud condensation nuclei (CCN) during new particle formation events, Geophys. Res. Lett., 37, L03804, doi:10.1029/2009gl040930, 2010.

Edney, E. O., Kleindienst, T. E., Jaoui, M., Lewandowski, M., Offenberg, J. H., Wang, W., and Claeys, M.: Formation of 2-methyl tetrols and 2-methylglyceric acid in secondary organic aerosol from laboratory irradiated isoprene/NO_x/SO_2/air mixtures and their detection in ambient $PM_{2.5}$ samples collected in the eastern United States, Atmos. Environ., 39, 5281–5289, doi:10.1016/j.atmosenv.2005.05.031, 2005.

Edwards, J. M. and Slingo, A.: Studies with a flexible new radiation code, I: Choosing a configuration for a large-scale model, Q. J. Roy. Meteor. Soc., 122, 689–719, doi:10.1002/qj.49712253107, 1996.

Engelhart, G. J., Asa-Awuku, A., Nenes, A., and Pandis, S. N.: CCN activity and droplet growth kinetics of fresh and aged monoterpene secondary organic aerosol, Atmos. Chem. Phys., 8, 3937–3949, doi:10.5194/acp-8-3937-2008, 2008.

Engelhart, G. J., Moore, R. H., Nenes, A., and Pandis, S. N.: Cloud condensation nuclei activity of isoprene secondary organic aerosol, J. Geophys. Res., 116, D02207, doi:10.1029/2010jd014706, 2011.

Fan, J., Zhang, R., Collins, D., and Li, G.: Contribution of secondary condensable organics to new particle formation: a case study in Houston, Texas, Geophys. Res. Lett., 33, L15802, doi:10.1029/2006gl026295, 2006.

Forster, P., Ramaswamy, V., Artaxo, P., Berntsen, T., Betts, R., Fahey, D. W., Haywood, J., Lean, J., Lowe, D. C., Myhre, G., Nganga, J., Prinn, R., Raga, G., Schulz, M., and Dorland, R. V.: Changes in atmospheric constituents and in radiative forcing, in: Climate Change 2007: The Physical Science Basis. Contribution of Working Group I to the Fourth Assessment Report of the Intergovernmental Panel on Climate Change, edited by: Solomon, S., Qin, D., Manning, M., Chen, Z., Marquis, M., Averyt, K. B., Tignor, M., and Miller, H. L., Cambridge University Press, Cambridge, UK and New York, USA, 2007.

Fountoukis, C. and Nenes, A.: Continued development of a cloud droplet formation parameterization for global climate models, J. Geophys. Res., 110, D11212, doi:10.1029/2004jd005591, 2005.

ACPD
13, 16961–17019, 2013

Fuchs, N. A. and Sutugin, A. G.: Highly dispersed aerosols, in: Topics in Current Aerosol Research, Pergamin, New York, 1–60, 1971.
Goldstein, A. H. and Galbally, I. E.: Known and unexplored organic constituents in the Earth's atmosphere, Environ. Sci. Technol., 41, 1514–1521, doi:10.1021/es072476p, 2007.
Gong, S. L.: A parameterization of sea-salt aerosol source function for sub- and super-micron particles, Global Biogeochem. Cy., 17, 1097, doi:10.1029/2003gb002079, 2003.
Goto, D., Takemura, T., and Nakajima, T.: Importance of global aerosol modeling including secondary organic aerosol formed from monoterpene, J. Geophys. Res., 113, D07205, doi:10.1029/2007jd009019, 2008.
Griffin, R. J., Cocker III, D. R., Seinfeld, J. H., and Dabdub, D.: Estimate of global atmospheric organic aerosol from oxidation of biogenic hydrocarbons, Geophys. Res. Lett., 26, 2721–2724, doi:10.1029/1999gl900476, 1999.
Guenther, A., Hewitt, C. N., Erickson, D., Fall, R., Geron, C., Graedel, T., Harley, P., Klinger, L., Lerdau, M., McKay, W. A., Pierce, T., Scholes, B., Steinbrecher, R., Tallamraju, R., Taylor, J., and Zimmerman, P.: A global model of natural volatile organic compound emissions, J. Geophys. Res., 100, 8873–8892, doi:10.1029/94jd02950, 1995.
Guibert, S., Snider, J. R., and Brenguier, J.-L.: Aerosol activation in marine stratocumulus clouds: 1. Measurement validation for a closure study, J. Geophys. Res., 108, 8628, doi:10.1029/2002jd002678, 2003.
Gunthe, S. S., King, S. M., Rose, D., Chen, Q., Roldin, P., Farmer, D. K., Jimenez, J. L., Artaxo, P., Andreae, M. O., Martin, S. T., and Pöschl, U.: Cloud condensation nuclei in pristine tropical rainforest air of Amazonia: size-resolved measurements and modeling of atmospheric aerosol composition and CCN activity, Atmos. Chem. Phys., 9, 7551–7575, doi:10.5194/acp-9-7551-2009, 2009.
Halmer, M. M., Schmincke, H. U., and Graf, H. F.: The annual volcanic gas input into the atmosphere, in particular into the stratosphere: a global data set for the past 100 years, J. Volcanol. Geoth. Res., 115, 511–528, doi:10.1016/s0377-0273(01)00318-3, 2002.
Hatakeyama, S., Izumi, K., Fukuyama, T., and Akimoto, H.: Reactions of ozone with α-pinene and β-pinene in air: yields of gaseous and particulate products, J. Geophys. Res.-Atmos., 94, 13013–13024, doi:10.1029/JD094iD10p13013, 1989.
Hatakka, J., Aalto, T., Aaltonen, V., Aurela, M., Hakola, H., Komppula, M., Laurila, T., Lihavainen, H., Paatero, J., Salminen, K., and Viisanen, Y.: Overview of the atmospheric research activities and results at Pallas GAW station, Boreal Environ. Res., 8, 365–383, 2003.

ACPD
13, 16961–17019, 2013

Heald, C. L., Ridley, D. A., Kreidenweis, S. M., and Drury, E. E.: Satellite observations cap the atmospheric organic aerosol budget, Geophys. Res. Lett., 37, L24808, doi:10.1029/2010gl045095, 2010.

Heald, C. L., Coe, H., Jimenez, J. L., Weber, R. J., Bahreini, R., Middlebrook, A. M., Russell, L. M., Jolleys, M., Fu, T.-M., Allan, J. D., Bower, K. N., Capes, G., Crosier, J., Morgan, W. T., Robinson, N. H., Williams, P. I., Cubison, M. J., DeCarlo, P. F., and Dunlea, E. J.: Exploring the vertical profile of atmospheric organic aerosol: comparing 17 aircraft field campaigns with a global model, Atmos. Chem. Phys., 11, 12673–12696, doi:10.5194/acp-11-12673-2011, 2011.

Hudson, J. G. and Frisbie, P. R.: Surface cloud condensation nuclei and condensation nuclei measurements at Reno, Nevada, Atmos. Environ. A, 25, 2285–2299, doi:10.1016/0960-1686(91)90104-F, 1991.

Jimenez, J. L., Canagaratna, M. R., Donahue, N. M., Prevot, A. S. H., Zhang, Q., Kroll, J. H., DeCarlo, P. F., Allan, J. D., Coe, H., Ng, N. L., Aiken, A. C., Docherty, K. S., Ulbrich, I. M., Grieshop, A. P., Robinson, A. L., Duplissy, J., Smith, J. D., Wilson, K. R., Lanz, V. A., Hueglin, C., Sun, Y. L., Tian, J., Laaksonen, A., Raatikainen, T., Rautiainen, J., Vaattovaara, P., Ehn, M., Kulmala, M., Tomlinson, J. M., Collins, D. R., Cubison, M. J., E., Dunlea, J., Huffman, J. A., Onasch, T. B., Alfarra, M. R., Williams, P. I., Bower, K., Kondo, Y., Schneider, J., Drewnick, F., Borrmann, S., Weimer, S., Demerjian, K., Salcedo, D., Cottrell, L., Griffin, R., Takami, A., Miyoshi, T., Hatakeyama, S., Shimono, A., Sun, J. Y., Zhang, Y. M., Dzepina, K., Kimmel, J. R., Sueper, D., Jayne, J. T., Herndon, S. C., Trimborn, A. M., Williams, L. R., Wood, E. C., Middlebrook, A. M., Kolb, C. E., Baltensperger, U., and Worsnop, D. R.: Evolution of organic aerosols in the atmosphere, Science, 326, 1525–1529, doi:10.1126/science.1180353, 2009.

Kanakidou, M., Seinfeld, J. H., Pandis, S. N., Barnes, I., Dentener, F. J., Facchini, M. C., Van Dingenen, R., Ervens, B., Nenes, A., Nielsen, C. J., Swietlicki, E., Putaud, J. P., Balkanski, Y., Fuzzi, S., Horth, J., Moortgat, G. K., Winterhalter, R., Myhre, C. E. L., Tsigaridis, K., Vignati, E., Stephanou, E. G., and Wilson, J.: Organic aerosol and global climate modelling: a review, Atmos. Chem. Phys., 5, 1053–1123, doi:10.5194/acp-5-1053-2005, 2005.

Kanawade, V. P., Jobson, B. T., Guenther, A. B., Erupe, M. E., Pressley, S. N., Tripathi, S. N., and Lee, S.-H.: Isoprene suppression of new particle formation in a mixed deciduous forest, Atmos. Chem. Phys., 11, 6013–6027, doi:10.5194/acp-11-6013-2011, 2011.

Kavouras, I. G., Mihalopoulos, N., and Stephanou, E. G.: Formation of atmospheric particles from organic acids produced by forests, Nature, 395, 683–686, doi:10.1038/27179, 1998.
Kavouras, I. G., Mihalopoulos, N., and Stephanou, E. G.: Formation and gas/particle partitioning of monoterpenes photo-oxidation products over forests, Geophys. Res. Lett., 26, 55–58, doi:10.1029/1998gl900251, 1999.
Kerminen, V.-M. and Kulmala, M.: Analytical formulae connecting the "real" and the "apparent" nucleation rate and the nuclei number concentration for atmospheric nucleation events, J. Aerosol Sci., 33, 609–622, doi:10.1016/s0021-8502(01)00194-x, 2002.
Kettle, A. J. and Andreae, M. O.: Flux of dimethylsulfide from the oceans: a comparison of updated data sets and flux models, J. Geophys. Res.-Atmos., 105, 26793–26808, doi:10.1029/2000jd900252, 2000.
Kiendler-Scharr, A., Wildt, J., Maso, M. D., Hohaus, T., Kleist, E., Mentel, T. F., Tillmann, R., Uerlings, R., Schurr, U., and Wahner, A.: New particle formation in forests inhibited by isoprene emissions, Nature, 461, 381–384, doi:10.1038/nature08292, 2009.
King, S. M., Rosenoern, T., Shilling, J. E., Chen, Q., Wang, Z., Biskos, G., McKinney, K. A., Pöschl, U., and Martin, S. T.: Cloud droplet activation of mixed organic-sulfate particles produced by the photooxidation of isoprene, Atmos. Chem. Phys., 10, 3953–3964, doi:10.5194/acp-10-3953-2010, 2010.
Komppula, M., Lihavainen, H., Hatakka, J., Paatero, J., Aalto, P., Kulmala, M., and Viisanen, Y.: Observations of new particle formation and size distributions at two different heights and surroundings in subarctic area in northern Finland, J. Geophys. Res.-Atmos., 108, 4295, doi:10.1029/2002jd002939, 2003.
Kroll, J. H., Ng, N. L., Murphy, S. M., Flagan, R. C., and Seinfeld, J. H.: Secondary organic aerosol formation from isoprene photooxidation under high-NO_x conditions, Geophys. Res. Lett., 32, L18808, doi:10.1029/2005gl023637, 2005.
Kroll, J. H., Ng, N. L., Murphy, S. M., Flagan, R. C., and Seinfeld, J. H.: Secondary organic aerosol formation from isoprene photooxidation, Environ. Sci. Technol., 40, 1869–1877, doi:10.1021/es0524301, 2006.
Kulmala, M., Laaksonen, A., and Pirjola, L.: Parameterisations for sulphuric acid/water nucleation rates, J. Geophys. Res.-Atmos., 103, 8301–8307, doi:10.1029/97JD03718, 1998a.
Kulmala, M., Toivonen, A., Mäkelä, J. M., and Laaksonen, A.: Analysis of the growth of nucleation mode particles observed in Boreal forest, Tellus B, 50, 449–462, doi:10.1034/j.1600-0889.1998.t01-4-00004.x, 1998b.

ACPD
13, 16961–17019, 2013

The direct and indirect radiative effects of biogenic SOA

C. E. Scott et al.

Kulmala, M., Hämeri, K., Aalto, P. P., Mäkelä, J. M., Pirjola, L., Nilsson, E. D., Buzorius, G., Rannik, Ü., Maso, M. D., Seidl, W., Hoffman, T., Janson, R., Hansson, H.-C., Viisanen, Y., Laaksonen, A., and O'Dowd, C. D.: Overview of the international project on biogenic aerosol formation in the boreal forest (BIOFOR), Tellus B, 53, 324–343, doi:10.1034/j.1600-0889.2001.530402.x, 2001a.

Kulmala, M., Maso, M. D., Mäkelä, J. M., Pirjola, L., Väkevä, M., Aalto, P., Miikkulainen, P., Hämeri, K., and O'Dowd, C. D.: On the formation, growth and composition of nucleation mode particles, Tellus B, 53, 479–490, doi:10.1034/j.1600-0889.2001.530411.x, 2001b.

Kulmala, M., Suni, T., Lehtinen, K. E. J., Dal Maso, M., Boy, M., Reissell, A., Rannik, Ü., Aalto, P., Keronen, P., Hakola, H., Bäck, J., Hoffmann, T., Vesala, T., and Hari, P.: A new feedback mechanism linking forests, aerosols, and climate, Atmos. Chem. Phys., 4, 557–562, doi:10.5194/acp-4-557-2004, 2004.

Kulmala, M., Lehtinen, K. E. J., and Laaksonen, A.: Cluster activation theory as an explanation of the linear dependence between formation rate of 3 nm particles and sulphuric acid concentration, Atmos. Chem. Phys., 6, 787–793, doi:10.5194/acp-6-787-2006, 2006.

Kulmala, M., Kontkanen, J., Junninen, H., Lehtipalo, K., Manninen, H. E., Nieminen, T., Petäjä, T., Sipilä, M., Schobesberger, S., Rantala, P., Franchin, A., Jokinen, T., Järvinen, E., Äijälä, M., Kangasluoma, J., Hakala, J., Aalto, P. P., Paasonen, P., Mikkilä, J., Vanhanen, J., Aalto, J., Hakola, H., Makkonen, U., Ruuskanen, T., Mauldin, R. L., Duplissy, J., Vehkamäki, H., Bäck, J., Kortelainen, A., Riipinen, I., Kurtén, T., Johnston, M. V., Smith, J. N., Ehn, M., Mentel, T. F., Lehtinen, K. E. J., Laaksonen, A., Kerminen, V.-M., and Worsnop, D. R.: Direct observations of atmospheric aerosol nucleation, Science, 339, 943–946, doi:10.1126/science.1227385, 2013.

Kurten, T., Kulmala, M., Maso, M. D., Suni, T., Reissell, A., Vehkamaki, H., Hari, P., Laaksonen, A., Viisanen, Y., and Vesala, T.: Estimation of different forest-related contributions to the radiative balance using observations in southern Finland, Boreal Environ. Res., 8, 275–285, 2003.

Laaksonen, A., Kulmala, M., O'Dowd, C. D., Joutsensaari, J., Vaattovaara, P., Mikkonen, S., Lehtinen, K. E. J., Sogacheva, L., Dal Maso, M., Aalto, P., Petäjä, T., Sogachev, A., Yoon, Y. J., Lihavainen, H., Nilsson, D., Facchini, M. C., Cavalli, F., Fuzzi, S., Hoffmann, T., Arnold, F., Hanke, M., Sellegri, K., Umann, B., Junkermann, W., Coe, H., Allan, J. D., Alfarra, M. R., Worsnop, D. R., Riekkola, M.-L., Hyötyläinen, T., and Viisanen, Y.: The role of VOC oxi-

ACPD
13, 16961–17019, 2013

dation products in continental new particle formation, Atmos. Chem. Phys., 8, 2657–2665, doi:10.5194/acp-8-2657-2008, 2008.
Lathière, J., Hauglustaine, D. A., De Noblet-Ducoudré, N., Krinner, G., and Folberth, G. A.: Past and future changes in biogenic volatile organic compound emissions simulated with a global dynamic vegetation model, Geophys. Res. Lett., 32, L20818, doi:10.1029/2005gl024164, 2005.
Lee, L. A., Carslaw, K. S., Pringle, K. J., and Mann, G. W.: Mapping the uncertainty in global CCN using emulation, Atmos. Chem. Phys., 12, 9739–9751, doi:10.5194/acp-12-9739-2012, 2012.
Lee, L. A., Pringle, K. J., Reddington, C. L., Mann, G. W., Stier, P., Spracklen, D. V., Pierce, J. R., and Carslaw, K. S.: The magnitude and causes of uncertainty in global model simulations of cloud condensation nuclei, Atmos. Chem. Phys. Discuss., 13, 6295–6378, doi:10.5194/acpd-13-6295-2013, 2013.
Lihavainen, H., Kerminen, V.-M., Tunved, P., Aaltonen, V., Arola, A., Hatakka, J., Hyvärinen, A., and Viisanen, Y.: Observational signature of the direct radiative effect by natural boreal forest aerosols and its relation to the corresponding first indirect effect, J. Geophys. Res., 114, D20206, doi:10.1029/2009jd012078, 2009.
Makkonen, R., Asmi, A., Kerminen, V.-M., Boy, M., Arneth, A., Guenther, A., and Kulmala, M.: BVOC-aerosol-climate interactions in the global aerosol-climate model ECHAM5.5-HAM2, Atmos. Chem. Phys., 12, 10077–10096, doi:10.5194/acp-12-10077-2012, 2012.
Mann, G. W., Carslaw, K. S., Spracklen, D. V., Ridley, D. A., Manktelow, P. T., Chipperfield, M. P., Pickering, S. J., and Johnson, C. E.: Description and evaluation of GLOMAP-mode: a modal global aerosol microphysics model for the UKCA composition-climate model, Geosci. Model Dev., 3, 519–551, doi:10.5194/gmd-3-519-2010, 2010.
Mann, G. W., Carslaw, K. S., Ridley, D. A., Spracklen, D. V., Pringle, K. J., Merikanto, J., Korhonen, H., Schwarz, J. P., Lee, L. A., Manktelow, P. T., Woodhouse, M. T., Schmidt, A., Breider, T. J., Emmerson, K. M., Reddington, C. L., Chipperfield, M. P., and Pickering, S. J.: Intercomparison of modal and sectional aerosol microphysics representations within the same 3-D global chemical transport model, Atmos. Chem. Phys., 12, 4449–4476, doi:10.5194/acp-12-4449-2012, 2012.
Merikanto, J., Spracklen, D. V., Mann, G. W., Pickering, S. J., and Carslaw, K. S.: Impact of nucleation on global CCN, Atmos. Chem. Phys., 9, 8601–8616, doi:10.5194/acp-9-8601-2009, 2009.

ACPD
13, 16961–17019, 2013

Metzger, A., Verheggen, B., Dommen, J., Duplissy, J., Prevot, A. S. H., Weingartner, E., Riipinen, I., Kulmala, M., Spracklen, D. V., Carslaw, K. S., and Baltensperger, U.: Evidence for the role of organics in aerosol particle formation under atmospheric conditions, P. Natl. Acad. Sci. USA, 107, 6646–6651, doi:10.1073/pnas.0911330107, 2010.

Nenes, A. and Seinfeld, J. H.: Parameterization of cloud droplet formation in global climate models, J. Geophys. Res., 108, 4415, doi:10.1029/2002JD002911, 2003.

O'Donnell, D., Tsigaridis, K., and Feichter, J.: Estimating the direct and indirect effects of secondary organic aerosols using ECHAM5-HAM, Atmos. Chem. Phys., 11, 8635–8659, doi:10.5194/acp-11-8635-2011, 2011.

O'Dowd, C. D., Aalto, P., Hmeri, K., Kulmala, M., and Hoffmann, T.: Aerosol formation: Atmospheric particles from organic vapours, Nature, 416, 497–498, doi:10.1038/416497a, 2002.

Paasonen, P., Nieminen, T., Asmi, E., Manninen, H. E., Petäjä, T., Plass-Dülmer, C., Flentje, H., Birmili, W., Wiedensohler, A., Hõrrak, U., Metzger, A., Hamed, A., Laaksonen, A., Facchini, M. C., Kerminen, V.-M., and Kulmala, M.: On the roles of sulphuric acid and low-volatility organic vapours in the initial steps of atmospheric new particle formation, Atmos. Chem. Phys., 10, 11223–11242, doi:10.5194/acp-10-11223-2010, 2010.

Paasonen, P., Asmi, A., Petaja, T., Kajos, M. K., Aijala, M., Junninen, H., Holst, T., Abbatt, J. P. D., Arneth, A., Birmili, W., van der Gon, H. D., Hamed, A., Hoffer, A., Laakso, L., Laaksonen, A., Richard Leaitch, W., Plass-Dulmer, C., Pryor, S. C., Raisanen, P., Swietlicki, E., Wiedensohler, A., Worsnop, D. R., Kerminen, V.-M., and Kulmala, M.: Warming-induced increase in aerosol number concentration likely to moderate climate change, Nat. Geosci., 6, 438–442, doi:10.1038/ngeo1800, 2013.

Pacifico, F., Folberth, G. A., Jones, C. D., Harrison, S. P., and Collins, W. J.: Sensitivity of biogenic isoprene emissions to past, present, and future environmental conditions and implications for atmospheric chemistry, J. Geophys. Res., 117, D22302, doi:10.1029/2012jd018276, 2012.

Peng, Y., Lohmann, U., and Leaitch, R.: Importance of vertical velocity variations in the cloud droplet nucleation process of marine stratus clouds, J. Geophys. Res., 110, D21213, doi:10.1029/2004jd004922, 2005.

Penner, J. E., Andreae, M., Annegarn, H., Barrie, L., Feichter, J., Hegg, D., Jayaraman, A., Leaitch, R., Murphy, D., Nganga, J., and Pitari, G.: Aerosols, their direct and indirect effects, in: Climate Change 2001: The Physical Science Basis. Contribution of Working Group I to the Third Assessment Report of the Intergovernmental Panel on Climate Change, edited by:

ACPD
13, 16961–17019, 2013

Houghton, J. T., Ding, Y., Griggs, D. J., Noguer, M., van der Linden, P. J., Dai, X., Maskell, K., and Johnson, C. A., Cambridge University Press, Cambridge, UK and New York, USA, 2001.
Petters, M. D. and Kreidenweis, S. M.: A single parameter representation of hygroscopic growth and cloud condensation nucleus activity, Atmos. Chem. Phys., 7, 1961–1971, doi:10.5194/acp-7-1961-2007, 2007.
Pierce, J. R. and Adams, P. J.: Uncertainty in global CCN concentrations from uncertain aerosol nucleation and primary emission rates, Atmos. Chem. Phys., 9, 1339–1356, doi:10.5194/acp-9-1339-2009, 2009.
Pierce, J. R., Riipinen, I., Kulmala, M., Ehn, M., Petäjä, T., Junninen, H., Worsnop, D. R., and Donahue, N. M.: Quantification of the volatility of secondary organic compounds in ultrafine particles during nucleation events, Atmos. Chem. Phys., 11, 9019–9036, doi:10.5194/acp-11-9019-2011, 2011.
Pierce, J. R., Leaitch, W. R., Liggio, J., Westervelt, D. M., Wainwright, C. D., Abbatt, J. P. D., Ahlm, L., Al-Basheer, W., Cziczo, D. J., Hayden, K. L., Lee, A. K. Y., Li, S.-M., Russell, L. M., Sjostedt, S. J., Strawbridge, K. B., Travis, M., Vlasenko, A., Wentzell, J. J. B., Wiebe, H. A., Wong, J. P. S., and Macdonald, A. M.: Nucleation and condensational growth to CCN sizes during a sustained pristine biogenic SOA event in a forested mountain valley, Atmos. Chem. Phys., 12, 3147–3163, doi:10.5194/acp-12-3147-2012, 2012.
Pringle, K. J., Carslaw, K. S., Spracklen, D. V., Mann, G. M., and Chipperfield, M. P.: The relationship between aerosol and cloud drop number concentrations in a global aerosol microphysics model, Atmos. Chem. Phys., 9, 4131–4144, doi:10.5194/acp-9-4131-2009, 2009.
Pringle, K. J., Carslaw, K. S., Fan, T., Mann, G. W., Hill, A., Stier, P., Zhang, K., and Tost, H.: A multi-model assessment of the impact of sea spray geoengineering on cloud droplet number, Atmos. Chem. Phys., 12, 11647–11663, doi:10.5194/acp-12-11647-2012, 2012.
Pye, H. O. T. and Seinfeld, J. H.: A global perspective on aerosol from low-volatility organic compounds, Atmos. Chem. Phys., 10, 4377–4401, doi:10.5194/acp-10-4377-2010, 2010.
Rap, A., Scott, C. E., Spracklen D. V., Bellouin, N., Forster, P. M., Carslaw, K. S., Schmidt, A., and Mann., G.: Natural aerosol direct and indirect radiative effects, Geophys. Res. Lett., 40, doi:10.1002/grl.50441, 2013.
Reddington, C. L., Carslaw, K. S., Spracklen, D. V., Frontoso, M. G., Collins, L., Merikanto, J., Minikin, A., Hamburger, T., Coe, H., Kulmala, M., Aalto, P., Flentje, H., Plass-Dülmer, C., Birmili, W., Wiedensohler, A., Wehner, B., Tuch, T., Sonntag, A., O'Dowd, C. D., Jennings, S. G., Dupuy, R., Baltensperger, U., Weingartner, E., Hansson, H.-C., Tunved, P., Laj, P., Selle-

ACPD
13, 16961–17019, 2013

gri, K., Boulon, J., Putaud, J.-P., Gruening, C., Swietlicki, E., Roldin, P., Henzing, J. S., Moerman, M., Mihalopoulos, N., Kouvarakis, G., Ždímal, V., Zíková, N., Marinoni, A., Bonasoni, P., and Duchi, R.: Primary versus secondary contributions to particle number concentrations in the European boundary layer, Atmos. Chem. Phys., 11, 12007–12036, doi:10.5194/acp-11-12007-2011, 2011.

Riccobono, F., Rondo, L., Sipilä, M., Barmet, P., Curtius, J., Dommen, J., Ehn, M., Ehrhart, S., Kulmala, M., Kürten, A., Mikkilä, J., Paasonen, P., Petäjä, T., Weingartner, E., and Baltensperger, U.: Contribution of sulfuric acid and oxidized organic compounds to particle formation and growth, Atmos. Chem. Phys., 12, 9427–9439, doi:10.5194/acp-12-9427-2012, 2012.

Riipinen, I., Pierce, J. R., Yli-Juuti, T., Nieminen, T., Häkkinen, S., Ehn, M., Junninen, H., Lehtipalo, K., Petäjä, T., Slowik, J., Chang, R., Shantz, N. C., Abbatt, J., Leaitch, W. R., Kerminen, V.-M., Worsnop, D. R., Pandis, S. N., Donahue, N. M., and Kulmala, M.: Organic condensation: a vital link connecting aerosol formation to cloud condensation nuclei (CCN) concentrations, Atmos. Chem. Phys., 11, 3865–3878, doi:10.5194/acp-11-3865-2011, 2011.

Riipinen, I., Yli-Juuti, T., Pierce, J. R., Petäjä, T., Worsnop, D. R., Kulmala, M., and Donahue, N. M.: The contribution of organics to atmospheric nanoparticle growth, Nat. Geosci., 5, 453–458, doi:10.1038/ngeo1499, 2012.

Roberts, G. C., Andreae, M. O., Zhou, J., and Artaxo, P.: Cloud condensation nuclei in the Amazon Basin: “marine” conditions over a continent?, Geophys. Res. Lett., 28, 2807–2810, doi:10.1029/2000gl012585, 2001.

Robinson, N. H., Hamilton, J. F., Allan, J. D., Langford, B., Oram, D. E., Chen, Q., Docherty, K., Farmer, D. K., Jimenez, J. L., Ward, M. W., Hewitt, C. N., Barley, M. H., Jenkin, M. E., Rickard, A. R., Martin, S. T., McFiggans, G., and Coe, H.: Evidence for a significant proportion of Secondary Organic Aerosol from isoprene above a maritime tropical forest, Atmos. Chem. Phys., 11, 1039–1050, doi:10.5194/acp-11-1039-2011, 2011.

Rossow, W. B. and Schiffer, R. A.: Advances in Understanding Clouds from ISCCP, B. Am. Meteorol. Soc., 80, 2261–2287, 1999.

Schmidt, A., Carslaw, K. S., Mann, G. W., Rap, A., Pringle, K. J., Spracklen, D. V., Wilson, M., and Forster, P. M.: Importance of tropospheric volcanic aerosol for indirect radiative forcing of climate, Atmos. Chem. Phys., 12, 7321–7339, doi:10.5194/acp-12-7321-2012, 2012.

ACPD
13, 16961–17019, 2013

Scott, C. E., Spracklen, D. V., Pierce, J. R., Riipinen, I., and D'Andrea, S. D.: Impact of volatility treatment on the indirect radiative effect of biogenic secondary organic aerosol, in preparation, 2013.

Shilling, J. E., Chen, Q., King, S. M., Rosenoern, T., Kroll, J. H., Worsnop, D. R., DeCarlo, P. F., Aiken, A. C., Sueper, D., Jimenez, J. L., and Martin, S. T.: Loading-dependent elemental composition of α-pinene SOA particles, Atmos. Chem. Phys., 9, 771–782, doi:10.5194/acp-9-771-2009, 2009.

Sihto, S.-L., Kulmala, M., Kerminen, V.-M., Dal Maso, M., Petäjä, T., Riipinen, I., Korhonen, H., Arnold, F., Janson, R., Boy, M., Laaksonen, A., and Lehtinen, K. E. J.: Atmospheric sulphuric acid and aerosol formation: implications from atmospheric measurements for nucleation and early growth mechanisms, Atmos. Chem. Phys., 6, 4079–4091, doi:10.5194/acp-6-4079-2006, 2006.

Smith, J. N., Dunn, M. J., VanReken, T. M., Iida, K., Stolzenburg, M. R., McMurry, P. H., and Huey, L. G.: Chemical composition of atmospheric nanoparticles formed from nucleation in Tecamac, Mexico: Evidence for an important role for organic species in nanoparticle growth, Geophys. Res. Lett., 35, L04808, doi:10.1029/2007gl032523, 2008.

Snyder, P. K., Delire, C., and Foley, J. A.: Evaluating the influence of different vegetation biomes on the global climate, Clim. Dynam., 23, 279–302, doi:10.1007/s00382-004-0430-0, 2004.

Spracklen, D. V., Pringle, K. J., Carslaw, K. S., Chipperfield, M. P., and Mann, G. W.: A global off-line model of size-resolved aerosol microphysics: II. Identification of key uncertainties, Atmos. Chem. Phys., 5, 3233–3250, doi:10.5194/acp-5-3233-2005, 2005a.

Spracklen, D. V., Pringle, K. J., Carslaw, K. S., Chipperfield, M. P., and Mann, G. W.: A global off-line model of size-resolved aerosol microphysics: I. Model development and prediction of aerosol properties, Atmos. Chem. Phys., 5, 2227–2252, doi:10.5194/acp-5-2227-2005, 2005b.

Spracklen, D. V., Bonn, B., and Carslaw, K. S.: Boreal forests, aerosols and the impacts on clouds and climate, Philos. T. R. Soc. A, 366, 4613–4626, doi:10.1098/rsta.2008.0201, 2008a.

Spracklen, D. V., Carslaw, K. S., Kulmala, M., Kerminen, V.-M., Sihto, S.-L., Riipinen, I., Merikanto, J., Mann, G. W., Chipperfield, M. P., Wiedensohler, A., Birmili, W., and Lihavainen, H.: Contribution of particle formation to global cloud condensation nuclei concentrations, Geophys. Res. Lett., 35, L06808, doi:10.1029/2007gl033038, 2008b.

ACPD
13, 16961–17019, 2013

Spracklen, D. V., Carslaw, K. S., Pöschl, U., Rap, A., and Forster, P. M.: Global cloud condensation nuclei influenced by carbonaceous combustion aerosol, Atmos. Chem. Phys., 11, 9067–9087, doi:10.5194/acp-11-9067-2011, 2011a.

Spracklen, D. V., Jimenez, J. L., Carslaw, K. S., Worsnop, D. R., Evans, M. J., Mann, G. W., Zhang, Q., Canagaratna, M. R., Allan, J., Coe, H., McFiggans, G., Rap, A., and Forster, P.: Aerosol mass spectrometer constraint on the global secondary organic aerosol budget, Atmos. Chem. Phys., 11, 12109–12136, doi:10.5194/acp-11-12109-2011, 2011b.

Stier, P., Feichter, J., Kinne, S., Kloster, S., Vignati, E., Wilson, J., Ganzeveld, L., Tegen, I., Werner, M., Balkanski, Y., Schulz, M., Boucher, O., Minikin, A., and Petzold, A.: The aerosol-climate model ECHAM5-HAM, Atmos. Chem. Phys., 5, 1125–1156, doi:10.5194/acp-5-1125-2005, 2005.

Tunved, P., Ström, J., and Hansson, H.-C.: An investigation of processes controlling the evolution of the boundary layer aerosol size distribution properties at the Swedish background station Aspvreten, Atmos. Chem. Phys., 4, 2581–2592, doi:10.5194/acp-4-2581-2004, 2004.

Tunved, P., Hansson, H.-C., Kerminen, V.-M., Strom, J., Maso, M. D., Lihavainen, H., Viisanen, Y., Aalto, P. P., Komppula, M., and Kulmala, M.: High natural aerosol loading over boreal forests, Science, 312, 261–263, doi:10.1126/science.1123052, 2006.

Tunved, P., Ström, J., Kulmala, M., Kerminen, V.-M., Dal Maso, M., Svenningson, B., Lunder, C., and Hansson, H.-C.: The natural aerosol over Northern Europe and its relation to anthropogenic emissions – implications of important climate feedbacks, Tellus B, 60, 473–484, doi:10.1111/j.1600-0889.2008.00363.x, 2008.

Twomey, S.: Influence of Pollution on Shortwave Albedo Clouds, J. Atmos. Sci., 34, 1149–1152, 1977.

van der Werf, G. R., Randerson, J. T., Collatz, G. J., Giglio, L., Kasibhatla, P. S., Arellano, A. F., Olsen, S. C., and Kasischke, E. S.: Continental-Scale Partitioning of Fire Emissions During the 1997 to 2001 El Niño/La Niña Period, Science, 303, 73–76, doi:10.1126/science.1090753, 2004.

Verheggen, B., Mozurkewich, M., Caffrey, P., Frick, G., Hoppel, W., and Sullivan, W.: α-pinene oxidation in the presence of seed aerosol?: Estimates of nucleation rates, growth rates, and yield, Environ. Sci. Technol., 41, 6046–6051, doi:10.1021/es070245c, 2007.

Vestin, A., Rissler, J., Swietlicki, E., Frank, G. P., and Andreae, M. O.: Cloud-nucleating properties of the Amazonian biomass burning aerosol: cloud condensation nuclei measurements and modeling, J. Geophys. Res.-Atmos., 112, D14201, doi:10.1029/2006jd008104, 2007.

ACPD
13, 16961–17019, 2013

Wang, J., Lee, Y.-N., Daum, P. H., Jayne, J., and Alexander, M. L.: Effects of aerosol organics on cloud condensation nucleus (CCN) concentration and first indirect aerosol effect, Atmos. Chem. Phys., 8, 6325–6339, doi:10.5194/acp-8-6325-2008, 2008.

Williams, E., Rosenfeld, D., Madden, N., Gerlach, J., Gears, N., Atkinson, L., Dunnemann, N., Frostrom, G., Antonio, M., Biazon, B., Camargo, R., Franca, H., Gomes, A., Lima, M., Machado, R., Manhaes, S., Nachtigall, L., Piva, H., Quintiliano, W., Machado, L., Artaxo, P., Roberts, G., Renno, N., Blakeslee, R., Bailey, J., Boccippio, D., Betts, A., Wolff, D., Roy, B., Halverson, J., Rickenbach, T., Fuentes, J., and Avelino, E.: Contrasting convective regimes over the Amazon: implications for cloud electrification, J. Geophys. Res.-Atmos., 107, 8082, doi:10.1029/2001jd000380, 2002.

Woodhouse, M. T., Mann, G. W., Carslaw, K. S., and Boucher, O.: Sensitivity of cloud condensation nuclei to regional changes in dimethyl-sulphide emissions, Atmos. Chem. Phys., 13, 2723–2733, doi:10.5194/acp-13-2723-2013, 2013.

Yli-Juuti, T., Nieminen, T., Hirsikko, A., Aalto, P. P., Asmi, E., Hõrrak, U., Manninen, H. E., Patokoski, J., Dal Maso, M., Petäjä, T., Rinne, J., Kulmala, M., and Riipinen, I.: Growth rates of nucleation mode particles in Hyytiälä during 2003–2009: variation with particle size, season, data analysis method and ambient conditions, Atmos. Chem. Phys., 11, 12865–12886, doi:10.5194/acp-11-12865-2011, 2011.

Yu, J., Cocker, D. R., Griffin, R. J., Flagan, R. C., and Seinfeld, J. H.: Gas-phase ozone oxidation of monoterpenes: gaseous and particulate products, J. Atmos. Chem., 34, 207–258, doi:10.1023/a:1006254930583, 1999a.

Yu, J., Griffin, R. J., Cocker III, D. R., Flagan, R. C., Seinfeld, J. H., and Blanchard, P.: Observation of gaseous and particulate products of monoterpene oxidation in forest atmospheres, Geophys. Res. Lett., 26, 1145–1148, doi:10.1029/1999gl900169, 1999b.

Zhang, Q., Jimenez, J. L., Canagaratna, M. R., Allan, J. D., Coe, H., Ulbrich, I., Alfarra, M. R., Takami, A., Middlebrook, A. M., Sun, Y. L., Dzepina, K., Dunlea, E., Docherty, K., DeCarlo, P. F., Salcedo, D., Onasch, T., Jayne, J. T., Miyoshi, T., Shimono, A., Hatakeyama, S., Takegawa, N., Kondo, Y., Schneider, J., Drewnick, F., Borrmann, S., Weimer, S., Demerjian, K., Williams, P., Bower, K., Bahreini, R., Cottrell, L., Griffin, R. J., Rautiainen, J., Sun, J. Y., Zhang, Y. M., and Worsnop, D. R.: Ubiquity and dominance of oxygenated species in organic aerosols in anthropogenically-influenced Northern Hemisphere midlatitudes, Geophys. Res. Lett., 34, L13801, doi:10.1029/2007GL029979, 2007.

Zhang, R., Wang, L., Khalizov, A. F., Zhao, J., Zheng, J., McGraw, R. L., and Molina, L. T.: Formation of nanoparticles of blue haze enhanced by anthropogenic pollution, P. Natl. Acad. Sci. USA, 106, 17650–17654, doi:10.1073/pnas.0910125106, 2009.

ACPD
13, 16961–17019, 2013

Table 1. BVOC reaction rates used in this study (Atkinson et al., 1989, 2006).

Reaction	Rate coefficient ($cm^3 s^{-1}$)
α-pinene + OH	$1.2 \times 10^{-11} \exp(444/T)$
α-pinene + O_3	$1.01 \times 10^{-15} \exp(-732/T)$
α-pinene + NO_3	$1.19 \times 10^{-12} \exp(490/T)$
isoprene + OH	$2.7 \times 10^{-11} \exp(390/T)$
isoprene + O_3	$1.0 \times 10^{-14} \exp(-1995/T)$
isoprene + NO_3	$3.15 \times 10^{-12} \exp(-450/T)$

ACPD
13, 16961–17019, 2013

Table 2. Summary of model simulations and global annual mean changes to N_3 (number concentration of particles > 3 nm diameter) at the surface, surface level CCN (0.2 % supersaturation) concentration, and CDNC at cloud height (approximately 900 hPa), with subsequent all-sky DRE and first AIE, relative to an equivalent control simulation including no BVOC emission.

Exp. No.	Description	BVOC included (Global production of SOA given in brackets ($Tg(SOA)\,yr^{-1}$))	ΔN_3 (cm^{-3})	ΔCCN (cm^{-3})	ΔCDNC (cm^{-3})	All-sky DRE ($W\,m^{-2}$)	First AIE ($W\,m^{-2}$)
1	**ACT**	None	–	–	–	–	–
2	BHN with Eq. (1) within the boundary layer	Mon (20.4)	−64.3 (−7.9 %)	+23.5 (+10.4 %)	+7.7 (+4.1 %)	**−0.10**	**−0.07**
3		Iso (16.6)	−43.1 (−5.3 %)	+19.3 (+8.5 %)	+5.9 (+3.2 %)	**−0.08**	**−0.06**
4		Mon + Iso (37.0)	−79.6 (−9.7 %)	+29.0 (+12.8 %)	+8.2 (+4.4 %)	**−0.18**	**−0.06**
5	**ACT_x0.5** 0.5 × SOA production yield*	Mon + Iso (18.5)	−56.7 (−6.9 %)	+22.1 (+9.7 %)	+7.1 (+3.8 %)	**−0.09**	**−0.07**
6	**ACT_x2** 2 × SOA production yield*	Mon + Iso (74.0)	−106.7 (−13.0 %)	+36.7 (+16.2 %)	+9.0 (+4.8 %)	**−0.33**	**−0.04**
7	**ACT_x5** 5 × SOA production yield*	Mon + Iso (185.1)	−145.5 (−17.8 %)	+48.0 (+21.1 %)	+9.3 (+5.0 %)	**−0.78**	**+0.01**
8	**ACT_noSOAage** No transfer of non-hydrophilic particles to the hydrophilic distribution via condensation of secondary organics	Mon + Iso (37.0)	−81.3 (−9.9 %)	+8.3 (+3.6 %)	+3.6 (+1.9 %)	**−0.14**	**−0.02**
9	**ACT_fast_age**	None	–	–	–	–	–
10	One soluble monolayer required to transfer non-hydrophilic particles to the hydrophilic distribution	Mon + Iso (37.0)	−81.5 (−9.9 %)	+21.8 (+8.9 %)	+4.9 (+2.5 %)	**−0.18**	**−0.02**

* Experiments 5–7 were repeated with 1750 emissions of BC, OC and SO_2 to examine the effect of altering the yield of SOA production in a pre-industrial atmosphere.

ACPD
13, 16961–17019, 2013

Table 2. Continued.

Exp. No.	Description	BVOC included (Global production of SOA given in brackets ($Tg(SOA)\,yr^{-1}$))	ΔN_3 (cm^{-3})	ΔCCN (cm^{-3})	$\Delta CDNC$ (cm^{-3})	All-sky DRE ($W\,m^{-2}$)	First AIE ($W\,m^{-2}$)
11 12	**ACT_BCOCsmall** Size distribution of primary BC and OC emissions set to AeroCom recommendation (Dentener et al., 2006).	None Mon + Iso (37.0)	– −55.8 (−5.0 %)	– +46.0 (+17.5 %)	– +10.4 (+5.2 %)	– **−0.18**	– **−0.12**
13 14	**BHN** Binary homogeneous nucleation only	None Mon (20.4)	– −1.7 (−0.4 %)	– +20.3 (+10.4 %)	– +5.8 (+3.5 %)	– **−0.10**	– **−0.05**
15 16	**Org1** BHN with Eq. (2) throughout the atmosphere	None Mon (20.4)	– +643.0 (+142 %)	– +88.1 (+45.2 %)	– +44.2 (+26.6 %)	– **−0.08**	– **−0.77**
17 18	**Org2** BHN with Eq. (3) throughout the atmosphere	None Mon (20.4)	– +188.0 (+22.0 %)	– +39.0 (+15.5 %)	– +14.3 (+7.2 %)	– **−0.10**	– **−0.22**
19 20	**ACT_1750** 1750 emissions of BC (wildfire, biofuel), POM (wildfire, biofuel) and SO_2 (wildfire, domestic) taken from Dentener et al. (2006).	None Mon + Iso (37.0)	– −127.3 (−21.1 %)	– +23.8 (+23.2 %)	– +12.8 (+12.6 %)	– **−0.18**	– **−0.19**
21 22	**Org1_1750** 1750 emissions of BC (wildfire, biofuel), POM (wildfire, biofuel) and SO_2 (wildfire, domestic) taken from Dentener et al. (2006).	None Mon (20.4)	– +437.3 (+171 %)	– +52.5 (+56.7 %)	– +34.9 (+37.9 %)	– **−0.12**	– **−0.95**

* Experiments 5–7 were repeated with 1750 emissions of BC, OC and SO_2 to examine the effect of altering the yield of SOA production in a pre-industrial atmosphere.

ACPD
13, 16961–17019, 2013

Table 3. Pearson correlation coefficient (R) between multi-annual monthly mean observed and simulated monthly mean N_{80} concentrations. The normalised mean bias (NMB, %) in surface CCN concentration between model and observations is also given for each simulation.

Simulation		Exp. No.	Pearson correlation coefficient (R)			
			Hyytiala, Finland Typical background for high-latitude Europe; forest location but influenced by European pollution [24°17′ E, 61°51′ N]	**Aspvreten, Sweden** Boreal forest location, mid-Sweden [17°23′ E, 58°48′ N]	**Pallas, Finland** Very remote location at northern border of boreal zone [24°7′ E, 67°58′ N]	NMB (%) against sub-set of CCN dataset
ACT	No SOA	1	0.31	0.13	0.13	−44.4
	0.5 × SOA	5	0.42	0.22	0.36	−16.4
	SOA	4	0.44	0.22	0.40	**−16.0**
	2 × SOA	6	0.41	0.19	0.35	−16.7
	5 × SOA	7	0.26	0.06	0.15	−17.2
	No ageing by SOA	8	0.44	0.21	0.42	−40.5
	Fast ageing	10	0.44	0.19	0.40	−16.5
	BC/OC small	12	0.50	0.33	0.35	+48.2
Org1	No SOA	15	0.09	−0.15	−0.04	−48.6
	SOA	16	**0.61**	**0.46**	**0.60**	+16.9
Org2	No SOA	17	0.37	0.16	0.14	−26.6
	SOA	18	0.60	0.43	0.57	+20.8

ACPD
13, 16961–17019, 2013

Table 4. Locations included in the subset of CCN observations taken from Spracklen et al. (2011a).

Location		Reference
Balbina, Amazon Basin	59.4° W, 1.9° S	Roberts et al. (2001)
Rondonia, Amazon Basin	61.9° W, 10.9° S	Williams et al. (2002)
Amazon Basin	73° W, 5° S and 63° W, 12° S	Andreae et al. (2004)
Fazenda Nossa, Amazon Basin	62.35° W, 10.8° S	Vestin et al. (2007)
Reno, USA	119.8° W, 39.5° N	Hudson and Frisbie (1991)
Lauder, New Zealand	169.7° E, 45° S	Delene and Deshler (2001)

ACPD
13, 16961–17019, 2013

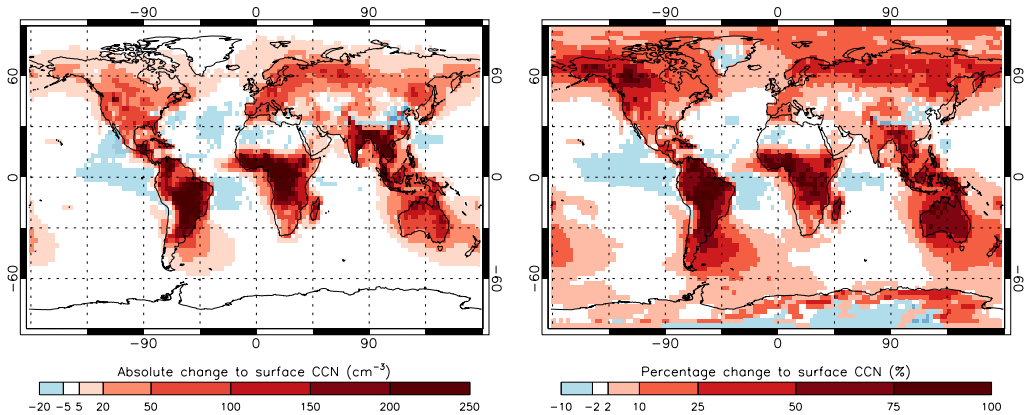

Fig. 1. Simulated annual mean absolute (left) and percentage (right) changes to surface cloud condensation nuclei (CCN) number concentration, calculated at 0.2 % supersaturation, resulting from the emission of both monoterpenes and isoprene when the ACT mechanism is used.

ACPD
13, 16961–17019, 2013

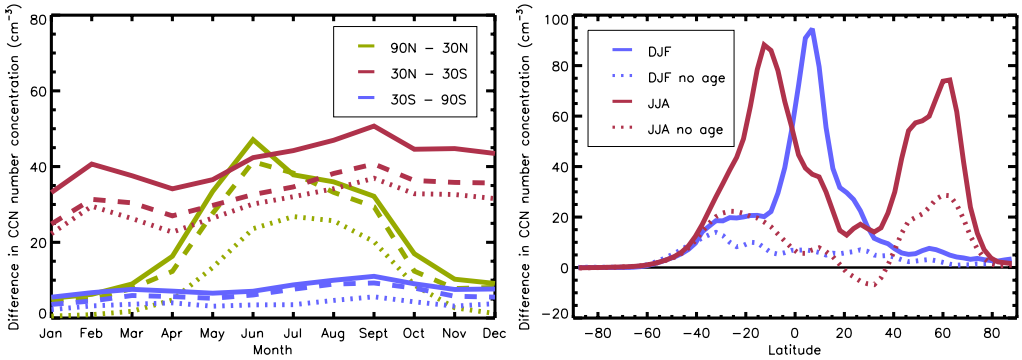

Fig. 2. Left: monthly mean absolute change in surface CCN number concentration (cm^{-3}) at 0.2 % supersaturation, across three latitude bands, when monoterpene (Expt. 2; dashed lines), isoprene (Expt.3; dotted lines) and both monoterpene and isoprene (Expt.4; solid lines) emissions are included in a simulation using the ACT mechanism. Right: seasonal mean absolute change in CCN number concentration (cm^{-3}) at 0.2 % supersaturation during December–February (blue) and June–August (red) using the ACT mechanism; Expt. 4 results (solid lines) include emissions of both monoterpenes and isoprene, Expt. 8 results (dotted lines) are equivalent but condensable organics do not transfer hydrophobic particles to the hydrophilic distribution.

ACPD
13, 16961–17019, 2013

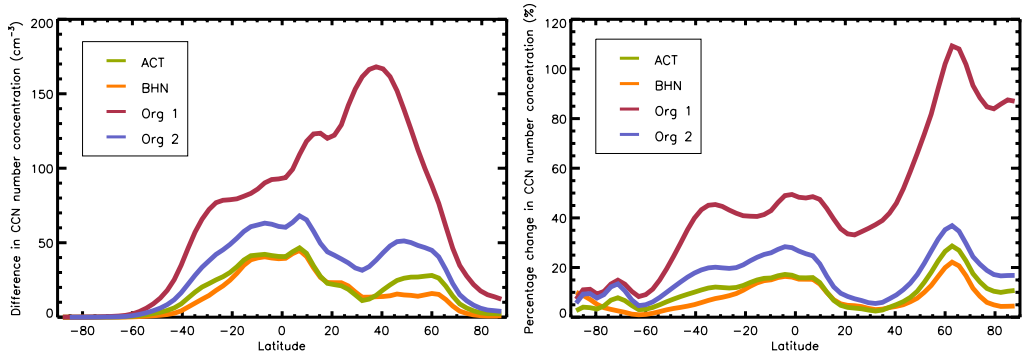

Fig. 3. Annual mean absolute change in surface CCN number concentration (left) and percentage change (right) at 0.2 % supersaturation for four particle formation mechanisms: ACT (green), BHN only (orange), Org1 (red) and Org2 (blue) from the emission of monoterpenes only.

ACPD
13, 16961–17019, 2013

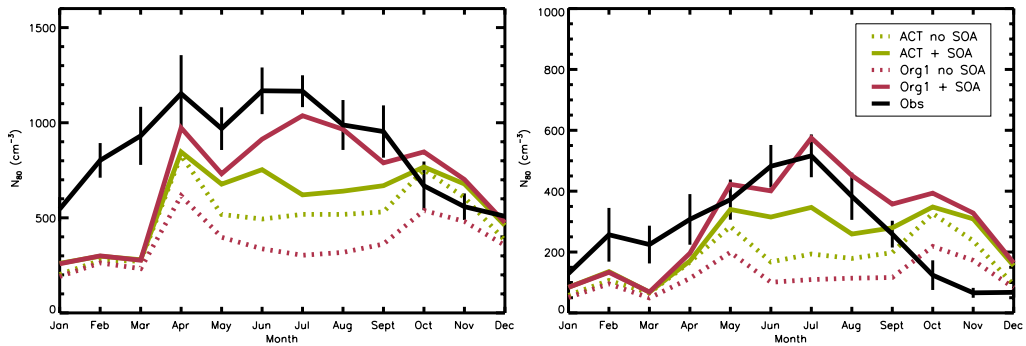

Fig. 4. Multi-annual monthly mean observed (black lines) seasonal cycle in N_{80} concentration at Hyytiala (left) and Pallas (right); standard deviation of the observed monthly mean is indicated by the vertical black lines. N_{80} concentrations simulated using the ACT (green; Expt.1 and Expt. 4) and Org1 (red; Expt. 15 and Expt. 16) nucleation mechanisms are shown with biogenic SOA (full lines) and without (dotted lines).

ACPD
13, 16961–17019, 2013

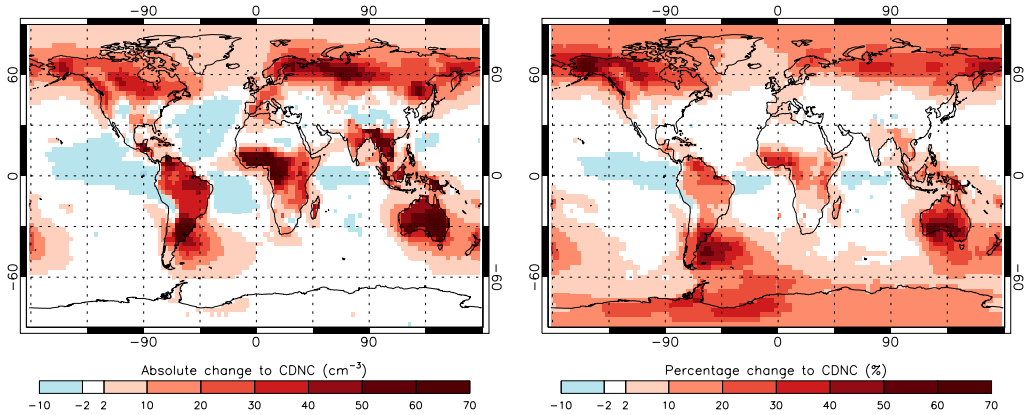

Fig. 5. Annual mean absolute (left) and percentage (right) change to CDNC due to biogenic SOA when the ACT nucleation mechanism is used (i.e. $[\mathrm{CDNC}]_{\mathrm{Expt.4}} - [\mathrm{CDNC}]_{\mathrm{Expt.1}}$).

ACPD
13, 16961–17019, 2013

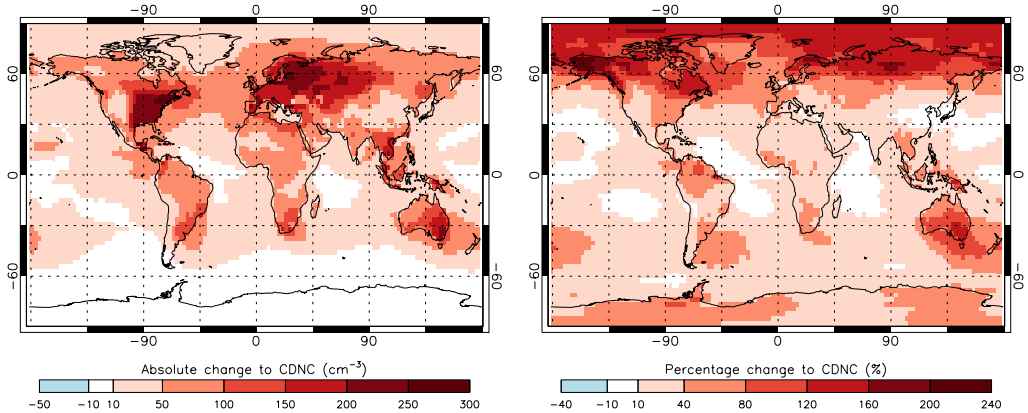

Fig. 6. Annual mean absolute (left) and percentage (right) change to CDNC due to biogenic SOA (monoterpenes only) when the Org1 nucleation mechanism is used (i.e. $[\mathrm{CDNC}]_{\mathrm{Expt.16}} - [\mathrm{CDNC}]_{\mathrm{Expt.15}}$).

ACPD
13, 16961–17019, 2013

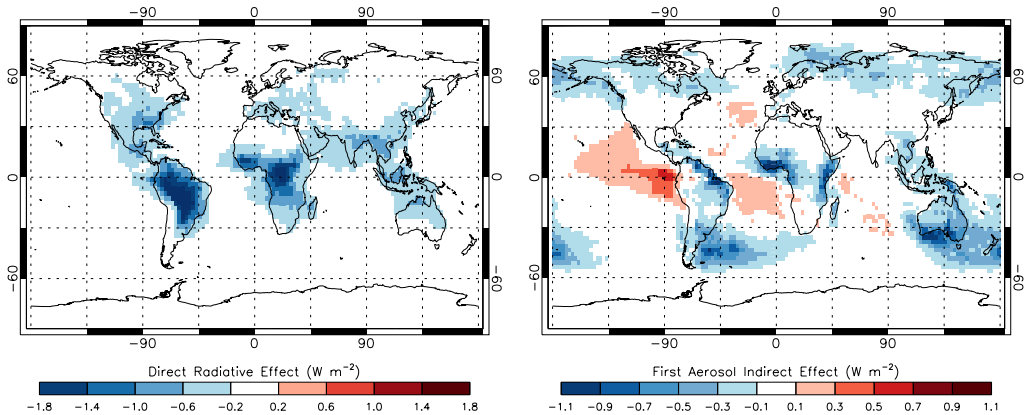

Fig. 7. Annual mean all-sky DRE (left), and first AIE (right) associated with the perturbation in cloud droplet number concentration, due to biogenic SOA (Expt. 4) relative to an equivalent simulation with no biogenic SOA (Expt. 1).

ACPD
13, 16961–17019, 2013

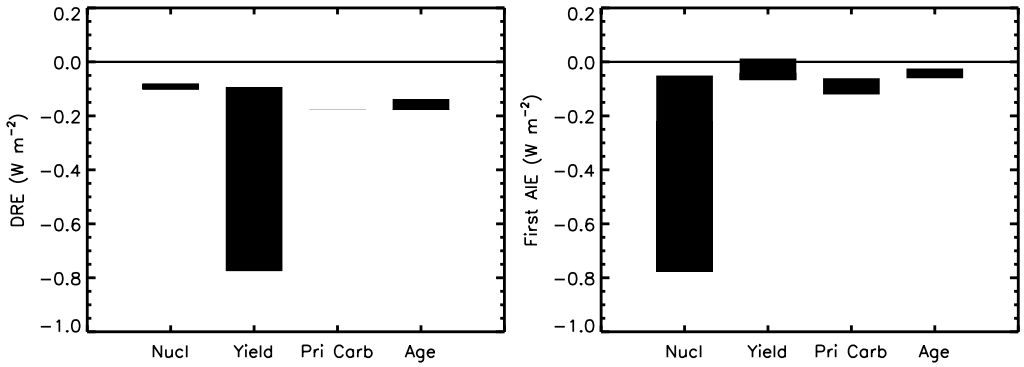

Fig. 8. Variation in global annual mean DRE (left) and AIE (right) of biogenic SOA associated with several parameters; black bars indicate the range of values obtained for each set of experiments: Nucl (nucleation mechanism; Expt. 2, 14, 16, 18), Yield (SOA yield; Expt. 4, 5, 6, 7), Pri Carb (primary carbonaceous emission size; Expt. 4, 12), Age (physical ageing; Expt. 4, 8, 10).

ACPD
13, 16961–17019, 2013

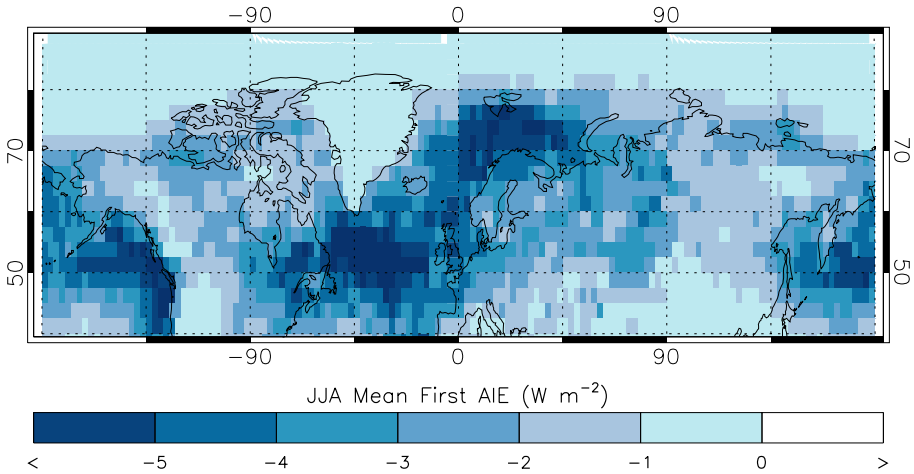

Fig. 9. Summertime (June-July-August) mean first AIE from monoterpene SOA when the Org1 nucleation mechanism is used (Expt. 16).

ACPD
13, 16961–17019, 2013

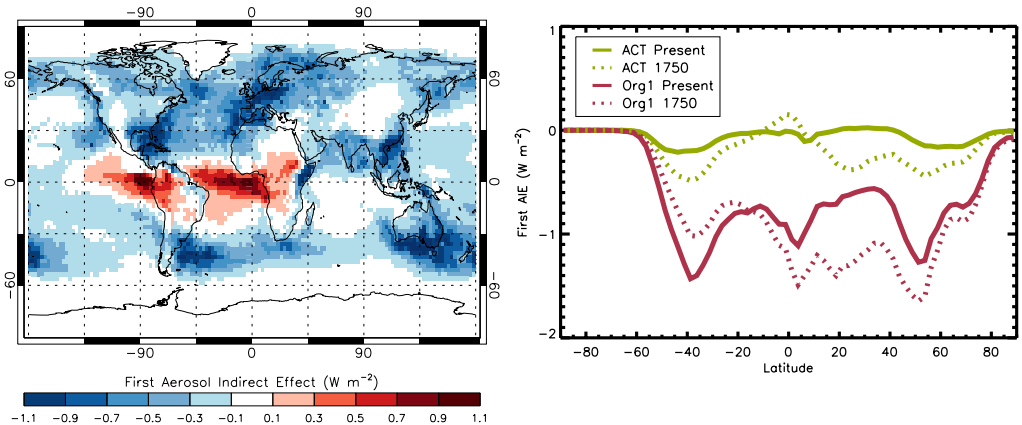

Fig. 10. Left: annual mean first AIE from biogenic SOA when anthropogenic emissions from 1750 are included in GLOMAP. Right: annual zonal mean AIE from biogenic SOA in the present day (solid lines) and pre-industrial (dashed lines) when the ACT (green) and Org1 (red) nucleation mechanisms are used.

ACPD
13, 16961–17019, 2013

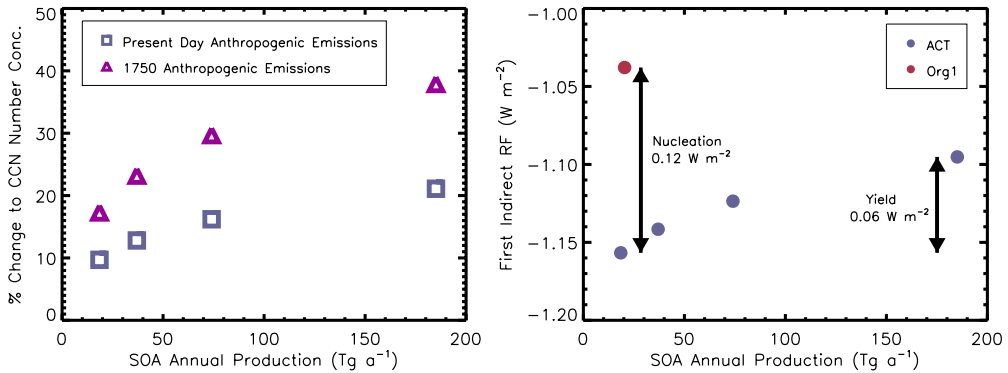

Fig. 11. Left: percentage change to global annual mean CCN concentration when biogenic SOA is included, simulated using the ACT nucleation mechanism at four different SOA production yields, with present day (squares) and pre-industrial (triangles) anthropogenic emissions. Right: anthropogenic first aerosol indirect RF from 1750 to present day, simulated using the ACT nucleation mechanism at four different yields for SOA production (purple circles), and using the Org1 nucleation mechanism with standard SOA production yield (red circle). Arrows highlight the RF sensitivity to assumptions about SOA yield and nucleation mechanism.

ACPD
13, 16961–17019, 2013